GEOSCIENCE FRONTIERS 3(6) (2012) 923–943

available at www.sciencedirect.com

China University of Geosciences (Beijing)

GEOSCIENCE FRONTIERS

journal homepage: www.elsevier.com/locate/gsf

RESEARCH PAPER

Protolith ages and timing of peak and retrograde metamorphism of the high-pressure granulites in the Shandong Peninsula, eastern North China Craton

Pinghua Liu, Fulai Liu*, Hong Yang, Fang Wang, Jianhui Liu

Institute of Geology, Chinese Academy of Geological Sciences, 26 Baiwanzhuang Road, Beijing 100037, China

Received 19 April 2011; received in revised form 22 November 2011; accepted 24 April 2012
Available online 2 May 2012

KEYWORDS
High-pressure granulite;
Zircon;
Mineral inclusions;
U-Pb geochronology;
Shandong Peninsula;
North China Craton

Abstract High-pressure (HP) granulites widely occur as enclaves within tonalite-trondhjemite-granodiorite (TTG) gneisses of the Early Precambrian metamorphic basement in the Shandong Peninsula, southeast part of the North China Craton (NCC). Based on cathodoluminescence (CL), laser Raman spectroscopy and in-situ U-Pb dating, we characterize the zircons from the HP granulites and group them into three main types: inherited (magmatic) zircon, HP metamorphic zircon and retrograde zircon. The inherited zircons with clear or weakly defined magmatic zoning contain inclusions of apatites, and $^{207}Pb/^{206}Pb$ ages of 2915–2890 Ma and 2763–2510 Ma, correlating with two magmatic events in the Archaean basement. The homogeneous HP metamorphic zircons contain index minerals of high-pressure metamorphism including garnet, clinopyroxene, plagioclase, quartz, rutile and apatite, and yield $^{207}Pb/^{206}Pb$ ages between 1900 and 1850 Ma, marking the timing of peak HP granulite facies metamorphism. The retrograde zircons contain inclusions of orthopyroxene, plagioclase, quartz, apatite and amphibole, and yield the youngest $^{207}Pb/^{206}Pb$ ages of 1840–1820 Ma among the three groups, which we correlate to the medium to low-pressure granulite facies retrograde metamorphism. The data presented in this study suggest subduction of Meso- and Neoarchean magmatic protoliths to lower crust depths where they were

* Corresponding author. Tel.: +86 10 68992873.
E-mail address: lfl0225@sina.com (F. Liu).

Peer-review under responsibility of China University of Geosciences (Beijing).
doi:10.1016/j.gsf.2012.04.001

subjected to HP granulite facies metamorphism during Palaeoproterozoic (1900–1850 Ma). Subsequently, the HP granulites were exhumated to upper crust levels, and were overprinted by medium to low-pressure granulite and amphibolite facies retrograde event at ca. 1840–820 Ma.

1. Introduction

Since the first report of high-pressure (HP) granulites from the Early Precambrian metamorphic basement in the North China Craton (NCC) by Wang et al. (1991) and Zhai et al. (1992), extensive investigations have been carried out in the past 20 years related to the nature of their protoliths, petrography, metamorphic conditions, and geochronology (Guo et al., 1993, 1998, 2002; Geng and Ji, 1994; Zhai et al., 1994; Ma and Wang, 1995; Liu et al., 1998, 2002; Wei et al., 2001; Zhao et al., 2001, 2003, 2005, 2009; Zhao, 2001, 2009; Zhai, 2004, 2009; Zhou et al., 2004, 2010; O'Brien et al., 2005; Zhang J. et al., 2006; Li et al., 2010, 2011; Zhai and Santosh, 2011, and references therein). Several studies also reported age data from the HP granulites and related rocks in the NCC including Guo et al. (2005), Kröner et al. (2005), Zhang H.F. et al. (2006), Zhang J. et al. (2006), Li and Zhao (2007), Luo et al. (2008), Guo and Li (2009), Wan et al. (2010), and Zhao et al. (2010). It has been suggested that the NCC witnessed HP granulite facies metamorphism between 1950 and 1850 Ma, when continent-continent collision occurred to form a unified cratonic metamorphic basement (Zhao et al., 2005, 2011). However, the HP granulites might have also experienced a retrograde metamorphic event following the peak HP conditions as suggested by the complex genetic types of zircons present in these rocks. Contrasting views exist on the zircon U-Pb ages from the HP granulites as to whether these represent peak high-pressure metamorphic conditions (Roberts and Finger, 1997; Ashwal et al., 1999; Whitehouse and Platt, 2003; Timmermann et al., 2004). Without careful identification of the mineral inclusions and microstructural data of the zircons based of laser Raman spectroscopy and cathodoluminescence (CL) imaging, it is difficult to estimate whether the U-Pb zircon ages of 1950–1850 Ma represent peak HP granulite facies metamorphism or not.

In this paper, we report results from a detailed investigation on zircons in HP granulites from the Shandong Peninsula, eastern China, involving mineral inclusion identification, CL imaging and U-Pb SIMS in-situ dating. Our results provide important insights on the timings of deposition (protolith) and metamorphism (peak HP and retrograde) based on we evaluate the evolution of the Early Precambrian metamorphic basement in the NCC. Mineral abbreviations are after Whitney and Evans (2010).

2. Geological setting

The Shandong Peninsula is located in the southeastern part of the NCC (Fig. 1), bordered by the Bohai Sea in the north, the West Shandong Terrain in the west with the Tan-Lu Fault forming the junction between the Sulu HP-UHP metamorphic belt in the southeast and bounded by the Yantai–Qingdao–Wulian Fault (Fig. 2). The major formations exposed in the Shandong Peninsula are Early Precambrian metamorphic rocks and Mesozoic plutonic rocks with minor Jurassic–Cretaceous continental

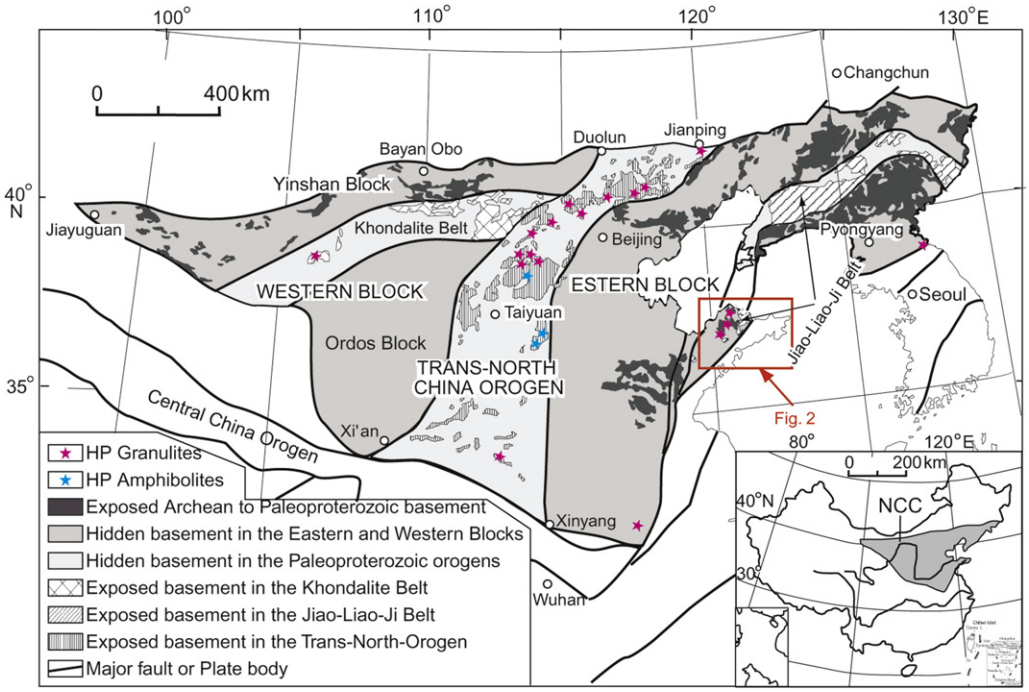

Figure 1 Tectonic subdivision of the Archaean to Palaeoproterozoic basement of the North China Craton and location of the high-pressure granulites (modified after Zhao et al., 2005, 2011).

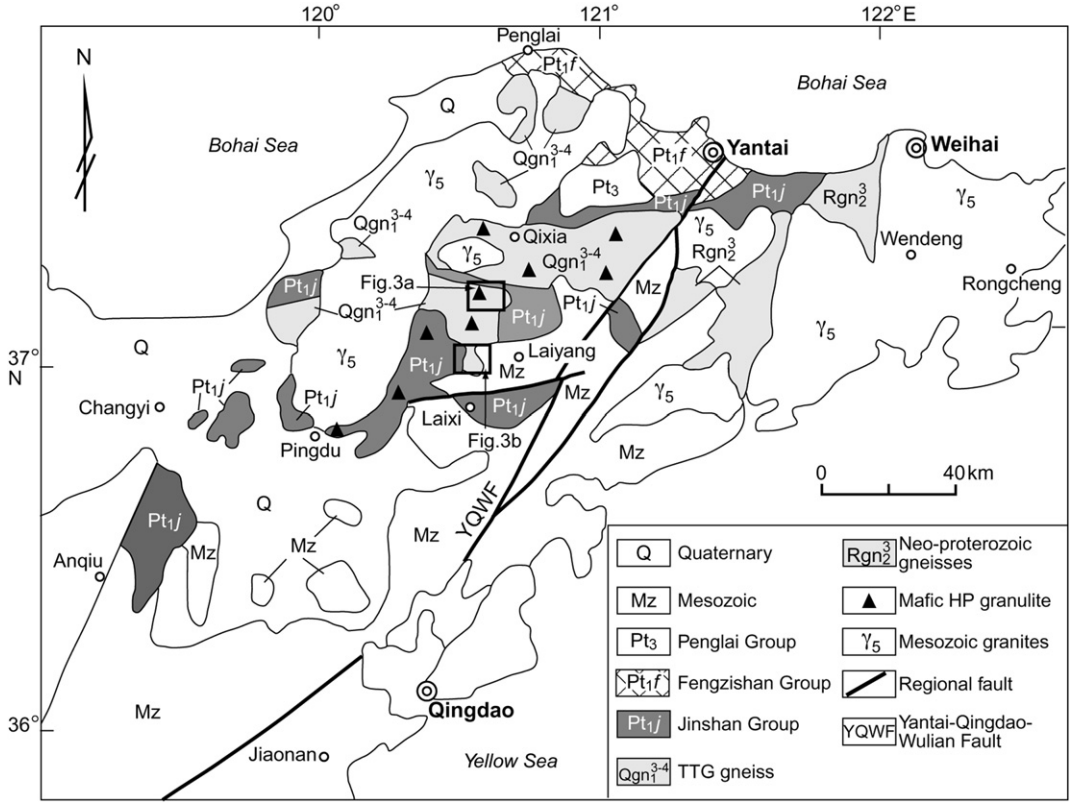

Figure 2 Simplified geological map and locations of HP granulites, Shandong Peninsula, eastern China (modified after Lu et al., 1996).

facies volcanic rocks, volcanic-sedimentary rocks and Tertiary basalts.

The Early Precambrian metamorphic rocks in the study area consist of Meso-Neoarchean tonalite-trondhjemite-granodiorite (TTG) gneisses, Palaeoproterozoic Khondalite Series rocks of the Jingshan and Fenzishan groups, Neoproterozoic metamorphic rocks of the Penglai Group, mafic-ultramafic rocks and HP granulites. The Meso-Neoarchean TTG gneisses are mainly located in the Qixia area. Previous studies indicate that protolithic ages of the TTG gneisses in the Shandong Peninsula can be subdivided into two groups, 2900–2700 Ma (Jahn et al., 2008) and ~2500 Ma (Tang et al., 2007; Zhou J.B. et al., 2008; Liu et al., 2011). The Palaeoproterozoic Khondalite Series of the Jingshan Group, located in Jingshan, Jingqishan and Nanshu in the Laiyang and Laixi area, have undergone amphibolite facies to granulite facies metamorphism (Zhou et al., 2004, 2007; Wang et al., 2009; Wang et al., 2010) to form biotite garnet sillimanite gneisses, marble, graphitic schist-gneisses, arkose-quartzite and biotite leptynite. The Khondalite Series of the Fenzishan Group, distributed in Miaohou and Menlou in the Qixia area, and Fenzishan in the Laizhou area, are represented by greenschist to lower amphibolite facies marble, biotite leptynite,

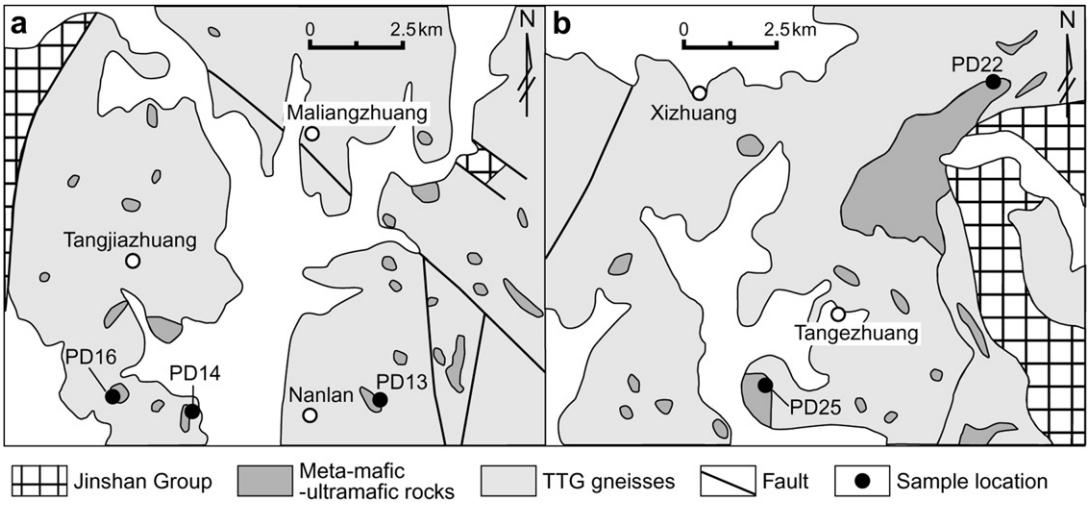

Figure 3 Simplified geological maps and sample locations of HP granulites in the study area, Shandong Peninsula. (a) Laixi; (b) Laiyang.

sillimanite biotite schist-gneisses and arkose-quartzite. SHRIMP U-Pb dating of metamorphic zircons from the Jingshan and Fenzishan group rocks shows metamorphic ages of 1950–1850 Ma (Wan et al., 2006). These ages are very similar to those of mafic HP granulites in the study area, indicating that the Early Precambrian metamorphic basement of Shandong Peninsula underwent a regional tectonic-thermal event in the Late Palaeoproterozoic (Liu et al., 1998, 2010; Zhou et al., 2004, 2008a,b; Hu et al., 2012). The Penglai Group rocks (mainly crystalline limestone, slate and quartzite) are exposed in the Penglai area and the northern part of the Qixia area, and have been metamorphosed only up to greenschist facies grade. Lenses of mafic-ultramafic rocks, HP granulites and amphibolites, discontinuously distributed in the TTG gneisses along the northeast-trending Pingdu–Laixi–Qixia belt, constitute a melange belt (Fig. 2). Bai et al. (1993) have noted that the melange is roughly parallel to the Sulu HP-UHP belt, and suggested that it might represent another HP-UHP metamorphic belt in the Shandong Peninsula; although subsequent petrological investigations indicated that this was not the case (Li et al., 1997; Liu et al., 1998, 2010). For the present study, five HP granulite samples were collected from the lenses of TTG gneisses near Buqian, Qianshanzhen and Nanlan in the northern Laixi area, and from Guandao in the Qixia area (Fig. 3).

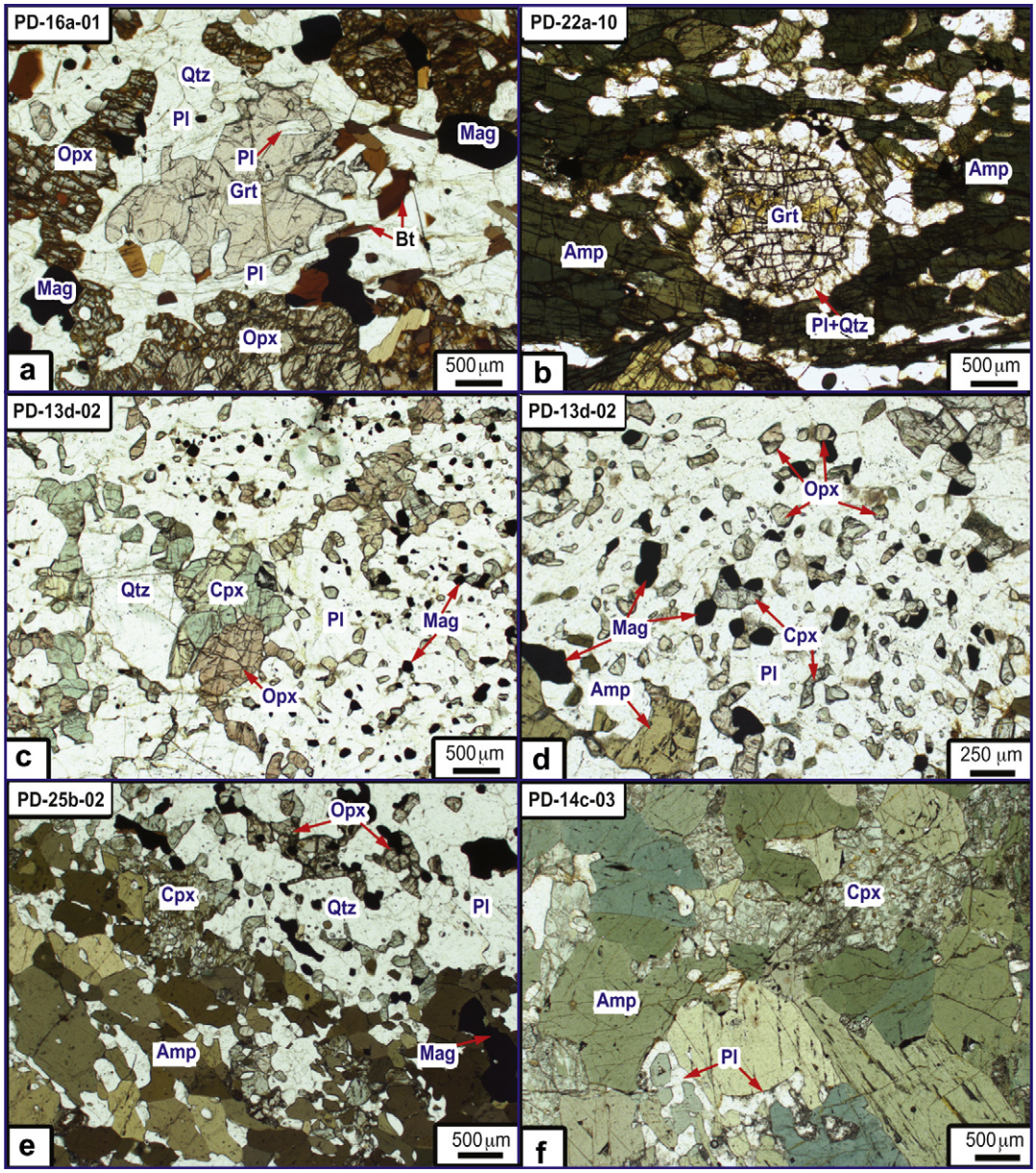

Figure 4 Photomicrographs (plane-polarized light) of mineral assemblages in the matrix of HP granulites, Shandong Peninsula. (a) Inclusions of plagioclase in relict garnet and symplectite of orthopyroxene + plagioclase + quartz surrounding relict garnet; (b) symplectite of amphibole + plagioclase + quartz surrounding relict garnet; (c) Amp-two-Px-granulite with clinopyroxene + orthopyroxene + plagioclase + quartz + Magnetite; (d) clinopyroxene + orthopyroxene + magnetite as fine inclusions in coarse plagioclase; (e) Amp-two-Px-granulite with clinopyroxene + orthopyroxene + amphibole + plagioclase + quartz + Magnetite; (f) Px-bearing amphibolite consisting of amphibole + plagioclase + clinopyroxene.

Table 1 Mineral inclusions in zircons from HP granulites, Shandong Peninsula.

Mineral inclusions	Retrogressive HP granulite		Amp-two-Px-granulite		Px-bearing amphibolite
	PD-16a-02	PD-22a-28	PD-13d-02	PD-25b-02	PD-14c-03
Garnet		*	*		
Clinopyroxene			*		*
Orthopyroxene	(*)				
Plagioclase	(*)	*	*	*	*
Quartz	(*)	*	*	*	*
Rutile			*		
Amphibole	(*)	*			
Apatite	(*)	*	*	*	(*)
Biotite				*	
Epidote				*	
Orpiment			(*)	*	
Magnetite			(*)	(*)	(*)
Ilmenite				(*)	
Chromite					(*)
Bismuthine				(*)	
Sphene		(*)		(*)	
Calcite		(*)		(*)	
Carbon dioxide					(*)

*Major phase; (*) Minor phase.

Granitoids (Linglong adamellite-granodiorite) emplaced within the Archaean TTG gneisses and the Jingshan Group metamorphic rocks in the study area are of Mesozoic Yanshanian age. Zircon $^{206}Pb/^{238}U$ ages range from 160 to 120 Ma (Wang and An, 1996; Miao et al., 1998; Wang et al., 1998).

3. Petrography

The five HP granulite samples examined in this study are Grt-Hy-granulite (PD-16a), Grt-amphibolite (PD-22a), Amp-two-Px-granulite (PD-13d and PD-25b), and Px-bearing amphibolite

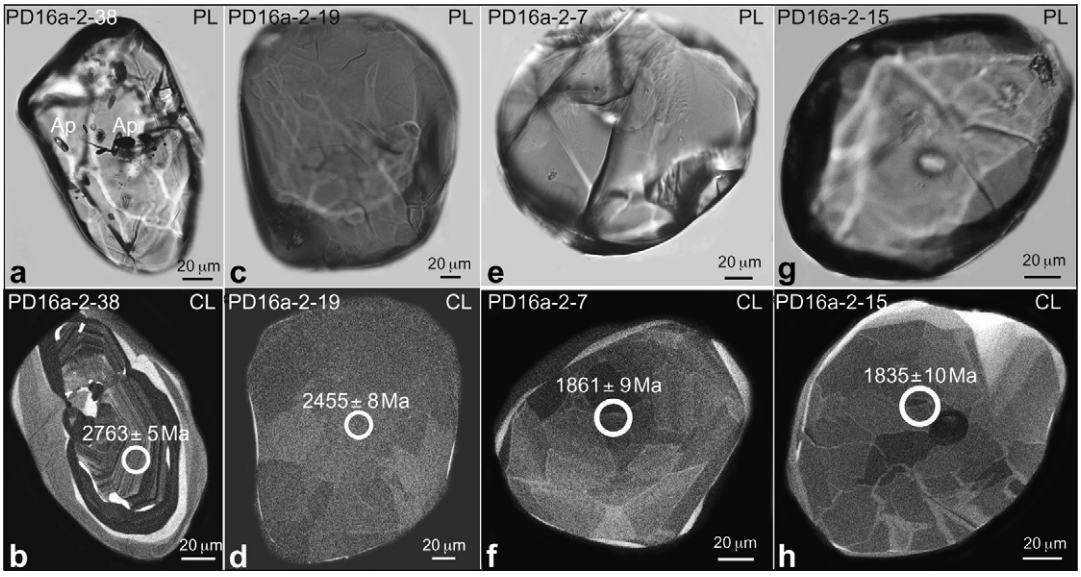

Figure 5 Plane-polarized light images of mineral inclusions, cathodoluminescence (CL) images and SIMS U-Pb ages of zircons from Grt-Hy-granulite (PD-16a-02). (a) Zircon grain (PD-16a-02-38) with inclusions of apatite (Ap) in both the inherited (magmatic) core and metamorphic rim; (b) CL image of the same zircon as (a) showing low-luminescent inherited (magmatic) core and middle-luminescent metamorphic rim, and a core $^{207}Pb/^{206}Pb$ age; (c) zircon (PD-16a-02-19) with no mineral inclusions; (d) CL image of the same metamorphic zircon as (c) showing a relatively homogeneous low-luminescent CL image, and a $^{207}Pb/^{206}Pb$ age; (e) small round zircon (PD-16a-02-7) with no mineral inclusions; (f) CL image of the same metamorphic zircon as (e) showing a high-luminescent CL image, and a $^{207}Pb/^{206}Pb$ age; (g) zircon (PD-16a-02-15) with no mineral inclusions; (h) CL image of the same metamorphic zircon as (g) showing a high-luminescent CL image, and a $^{207}Pb/^{206}Pb$ age.

(PD-14c). All these rocks show effects of retrograde metamorphism.

The Grt-Hy-granulite (PD16a-01) shows an assemblage of orthopyroxene, plagioclase, garnet, quartz and magnetite, with minor biotite, amphibole and K-feldspar, and accessory rutile, apatite and zircon. Relict garnet is surrounded by a symplectite of Opx + Pl + Qtz, some of which are locally replaced by a worm-like symplectite (Fig. 4a). The orthopyroxene is hypersthene (Liu et al., 2010).

Grt-amphibolite (PD22a-10) consists of amphibole, plagioclase and garnet, with minor quartz and magnetite, and accessory ilmenite, rutile, apatite and zircon. A fine-grained symplectite of Amp + Pl + Qtz surrounds garnet porphyroblasts, which is typical of 'white-eye circle' texture (Fig. 4b).

The main mineral assemblages of the Amp-two-Px-granulites (PD-13d-02, PD-25b-02) are clinopyroxene, orthopyroxene, amphibole, plagioclase and quartz, with minor biotite, ilmenite and magnetite. Rutile, apatite and zircon are accessory phases. Fine-grained intergrowths of orthopyroxene, clinopyroxene and amphibole occur (Fig. 4c–e), and coarse-grained clinopyroxene contains needles, laths or droplet-like crystals of plagioclase and quartz.

Px-bearing amphibolite (PD-14c-03) mainly consists of amphibole, plagioclase and clinopyroxene, with accessory ilmenite, rutile, apatite and zircon (Fig. 4f). Amphiboles occur as coarse and fine-grained varieties. Coarse-grained amphibole coexists with coarse-grained plagioclase and clinopyroxene. Fine-grained amphibole occurs as inclusions in coarse-grained clinopyroxene and plagioclase.

4. Analytical techniques

Zircons from the five HP granulites were separated using standard heavy-liquid and magnetic techniques, and then handpicked under a binocular microscope in the Mineral Separation Laboratory of the Institute of Regional Geological Survey in Langfang, Hebei Province. The selected crystals, together with the zircon standard TEMORA 1 (Black et al., 2003) were embedded in 25 mm epoxy discs and ground to approximately half their thickness. Mineral inclusions in zircon grains were identified by Laser Raman spectroscopy (RANISHAW RM-1000) at the Key Laboratory of Continental Dynamics, Ministry of Land and Mineral Resources, Beijing, China. Results of Laser Raman spectroscopy and analysis of mineral inclusions in zircon are listed in Table 1. Cathodoluminescence (CL) images of zircon grains were obtained at the Beijing SHRIMP Centre, Chinese Academy of Geological Sciences. The zircons were analyzed for U-Th-Pb isotope ratios using a SHRIMP (Sensitive High Resolution Ion Micro-Probe) II at the Beijing SHRIMP Centre, Chinese Academy of Geological Sciences, and a CAMECA IMS-1280 at the Ion Probe Laboratory of Geological and Geophysical Institute, using the procedures described by Song et al. (2002) and Li et al. (2009).

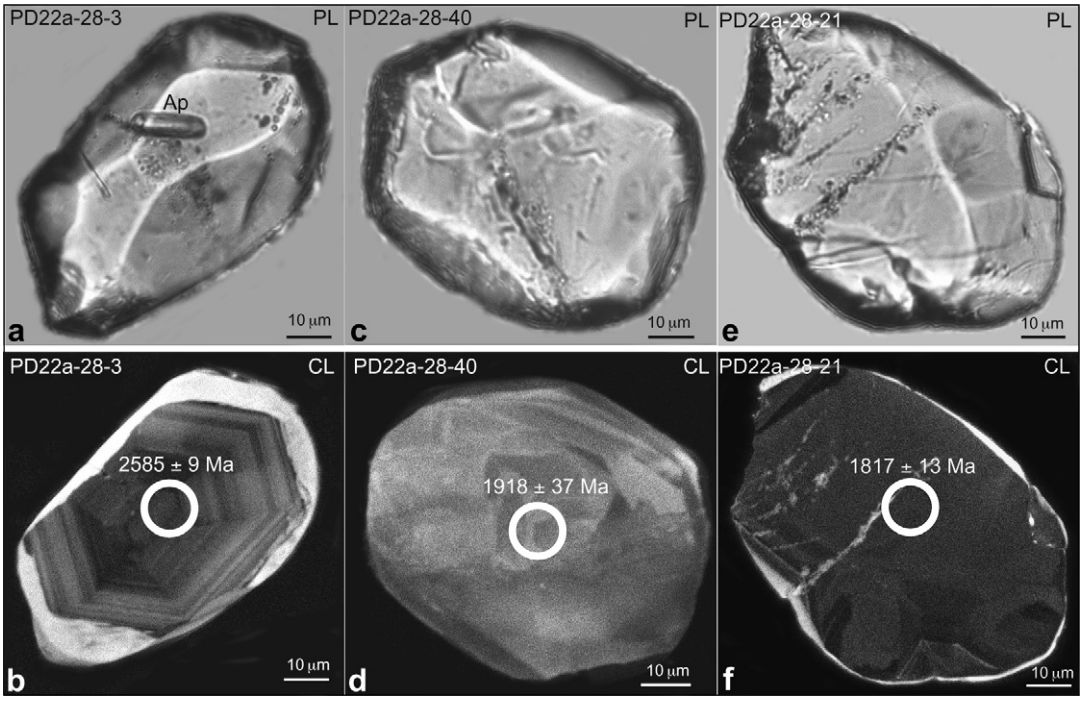

Figure 6 Plane-polarized light (PL) images of mineral inclusions, cathodoluminescence (CL) images and SIMS U-Pb ages of host zircons from Grt-amphibolite (PD-22a-28). (a) Zircon (PD-22a-28-3) with apatite inclusions in the inherited (magmatic) core and with no mineral inclusions in the metamorphic rim; (b) CL image of the same zircon as (a) showing low-luminescent inherited magmatic core and high-luminescent metamorphic rim, and a $^{207}Pb/^{206}Pb$ age; (c) zircon (PD-22a-28-40) with no mineral inclusions; (d) CL image of the same metamorphic zircon as (c) showing a middle-luminescent CL image, and a $^{207}Pb/^{206}Pb$ age; (e) zircon (PD-22a-28-21) with no mineral inclusions; (f) CL image of the same metamorphic zircon as (e) showing a low-luminescent CL image, and a $^{207}Pb/^{206}Pb$ age.

5. Mineral inclusions and cathodoluminescence (CL) imaging

5.1. Grt-Hy-granulite (PD-16a-02)

Zircons from Grt-Hy-granulite (sample PD-16a-02) are dark purplish red with size ranging from 50 to 300 μm (Fig. 5). Based on CL imaging, crystal habit and mineral inclusions, the zircons can be subdivided into four groups. *Group one* is characterized by low-luminescent inherited (magmatic) cores surrounded by relatively high-luminescent metamorphic rims. Widths of the rims are quite variable, ranging from a few to more than 100 μm. Luminescence of the rims is homogeneous indicating a typical metamorphic origin. Laser Raman spectroscopy indicates the presence of rare mineral inclusions in cores and rims. Zircons of *group two* are anhedral or nearly rounded and characterized by homogeneous low-luminescence with rare mineral inclusions (Table 1; Fig. 5c). CL image features and the crystal habit of *group two* zircons indicate a metamorphic origin. *Group three* zircons have high-luminescence and contain a few inclusions of quartz, apatite and amphibole (Table 1; Fig. 5f). Zircons of *group four* are rounded with high-luminescence. Only a few mineral inclusions (Opx + Pl + Qtz + Ap + Amp) are present, which are the same as the low to moderate pressure granulite facies assemblage in the host rock (Fig. 5g and h).

5.2. Grt-amphibolite (PD-22a-28)

Zircon grains from Grt-amphibolite PD-22a-28 are purplish red and subeuhedral with grain lengths of 20–250 μm (Fig. 6). Zircon can be subdivided into three groups. *Group one* has low-luminescent inherited (magmatic) cores surrounded by high-luminescent metamorphic rims. The inherited cores contain rare mineral inclusions such as apatite (Fig. 6a and b). CL images of some cores are blurry, indicating later heating. Widths of rims are highly variable and contain rare inclusions of garnet, plagioclase, quartz and amphibole, indicating that the overgrowth rims formed during the amphibolite facies metamorphism (Fig. 6c and d). *Group two* zircons exhibit homogeneous middle-luminescent CL images (Fig. 6c and d) and are devoid of mineral inclusions. Zircon grains of *group three* are characterized by low-luminescent CL images (Fig. 6e and f) and contain abundant inclusions of garnet, plagioclase, quartz and amphibole with minor titanite. The mineral inclusions in zircons of *group three* are quite similar to the assemblage of the host rock that indicates a retrograde amphibolite facies metamorphic overprint (Fig. 6e and f).

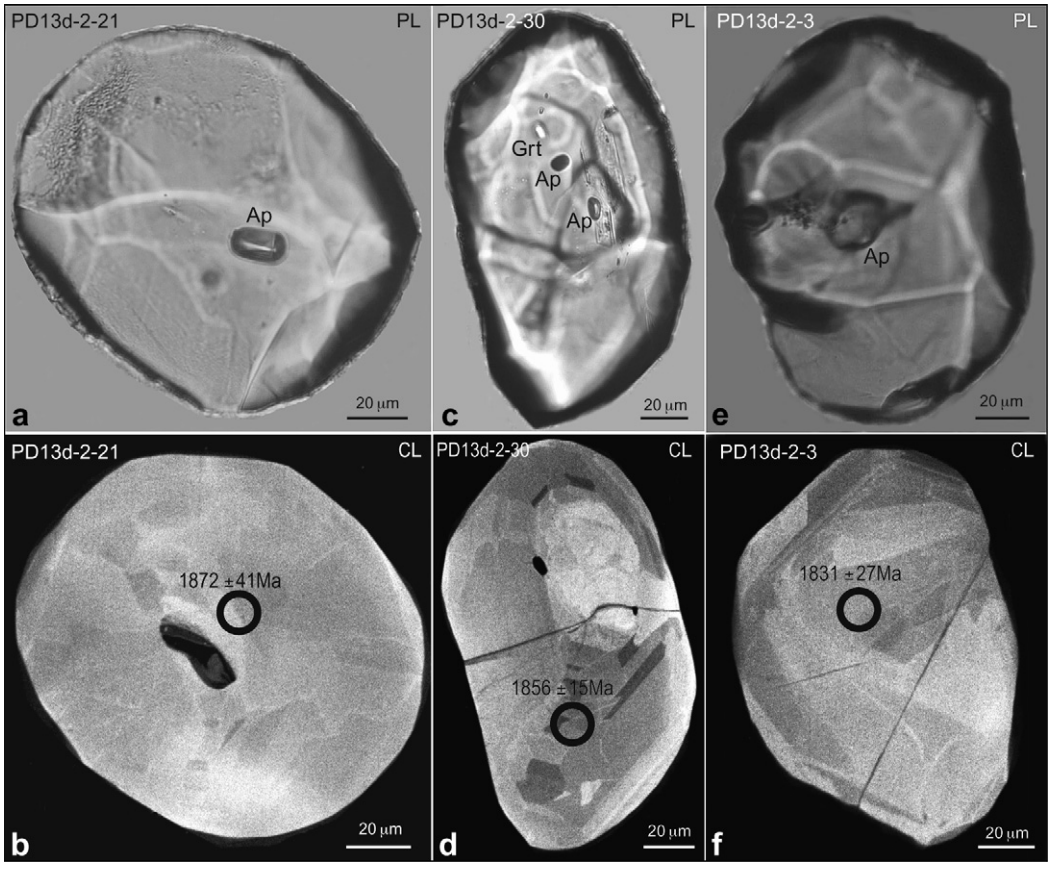

Figure 7 Plane-polarized light (PL) images of mineral inclusions, cathodoluminescence (CL) images and SIMS U-Pb ages of zircons from Amp-two-Px-granulite (PD-13d-02). (a) Zircon (PD-13d-02-21) with apatite inclusions; (b) CL image of the same metamorphic zircon as (a) showing a high-luminescent CL image, and a $^{207}Pb/^{206}Pb$ age; (c) zircon (PD-13d-02-30) with inclusions of Grt + Ap; (d) CL image of the same metamorphic zircon as (c) showing a high-luminescent CL image, and a $^{207}Pb/^{206}Pb$ age; (e) zircon (PD-13d-02-3) containing apatite inclusions; (f) CL image of the same metamorphic zircon as (e) showing a high-luminescent CL image, and a $^{207}Pb/^{206}Pb$ age.

5.3. Amp-two-Px-granulite (PD-13d-02 and PD-25b-02)

Although samples PD-13d-02 and PD-25b-02 are Amp-two-Px-granulites, there are notable differences in the CL images, crystal habit and mineral inclusions in their zircons. Zircons from sample PD-13d-02 are rounded with high-luminescent CL images, suggesting that they formed during granulite facies metamorphism (Fig. 7). A large number of mineral inclusions in zircons from PD-13d-02 consist of garnet, clinopyroxene, plagioclase, quartz, rutile and apatite. The inclusion assemblage indicates that Amp-two-Px-granulite (PD-13d-02) has undergone early HP granulite facies metamorphism.

Zircons from PD-25b-02 are relatively complex and belong to three groups. *Group one* zircons have low-luminescent inherited (magmatic) cores surrounded by high-luminescent metamorphic rims (Fig. 8a and b). There are only a few mineral inclusions except apatite in cores and rims (Fig. 8a and b). *Group two* zircons have medium-luminescent inherited (magmatic) cores surrounded by high-luminescent metamorphic rims (Fig. 8c and d). Cores of this group have abundant mineral inclusions composed of plagioclase, quartz, apatite, biotite epidote and orpiment. Homogeneous metamorphic rims contain no mineral inclusions (Fig. 8c and d). Zircons of *group three* are characterized by homogeneous high to medium-luminescent CL images without any mineral inclusions. Some zircon grains show fir-tree sector zoning, suggesting a granulite facies metamorphic origin (Vavra et al., 1996) (Fig. 8e–h).

5.4. Px-bearing amphibolite (PD-14c-03)

Zircons from Px-bearing amphibolite (sample PD-14c-03) are dark purplish red with size ranging from 50 to 300 μm. They are subdivided into two groups. *Group one* has low-luminescent inherited (magmatic) cores and high-luminescent metamorphic rims. The cores contain a few inclusions of quartz, plagioclase and clinopyroxene. In contrast, the rims have no mineral inclusions (Fig. 9a and b). *Group two* has homogeneous high-luminescent CL images with rounded grain habit. Zircons from *group two* also preserve similar mineral inclusions of quartz, plagioclase and clinopyroxene (Table 1; Fig. 9c–f).

6. U-Pb SIMS zircon dating

The results of 181 U-Pb SIMS analyses on 178 zircon grains from Grt-Hy-granulite PD-16a-02, Grt-amphibolite PD-22a-28, Amp-two-Px-granulite PD13d-02 and PD-25b-02, and Px-bearing amphibolite PD-14c-03 are summarized in Tables 2–6, and plotted on $^{207}Pb/^{235}U$ - $^{206}Pb/^{238}U$ diagrams with 1σ errors (Figs. 10–14).

6.1. Grt-Hy-granulite (PD-16a-02)

U-Pb SIMS analyses of zircons from PD-16a-02 define four discrete age groups (Table 2; Fig. 10). Five pre-metamorphic inherited (magmatic) cores with high Th/U ratios (0.67–1.65) yielded apparent $^{207}Pb/^{206}Pb$ ages ranging from 2763 ± 5 to 2652 ± 8 Ma. This age group is similar to $^{207}Pb/^{206}Pb$ ages of 2700–2600 Ma recorded by the inherited (magmatic) cores from the TTG gneisses and Grt-pyroxenite in the study area, which represent protolith ages of Grt-Hy-granulite PD-16a-02 and indicate an important magmatic event in the Late Neoarchean (Wan et al., 2006; Jahn et al., 2008; Tam et al., 2011). Nine spot analyses on metamorphic zircons characterized by low Th/U ratios

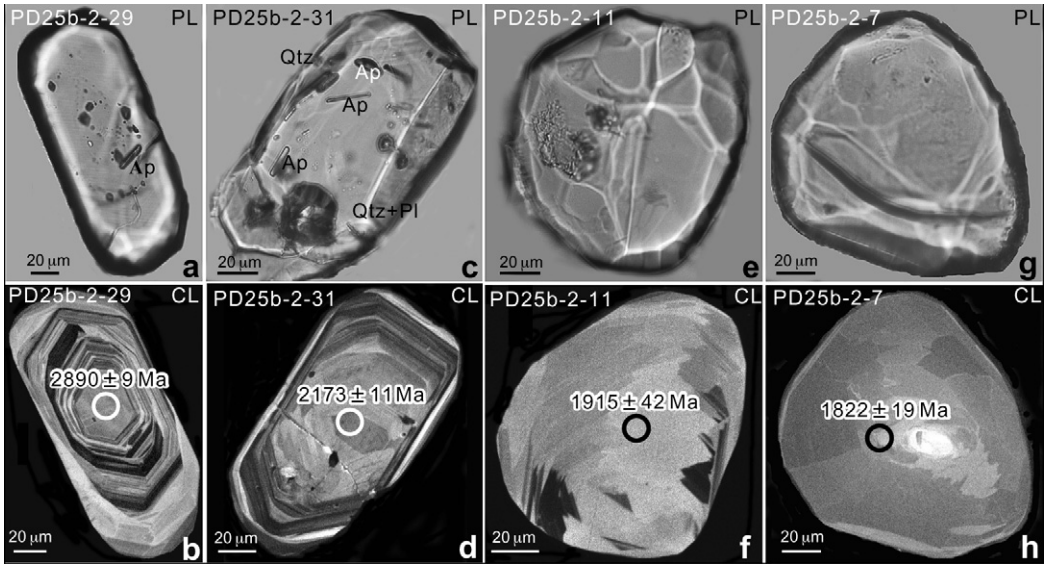

Figure 8 Plane-polarized light (PL) images of mineral inclusions, cathodoluminescence (CL) images and SIMS U-Pb ages of zircons from Amp-two-Px-granulite (PD-25b-02). (a) Zircon (PD-25b-02-29) contains apatite inclusions in the inherited magmatic core and has no mineral inclusions in the rim; (b) CL image of the same zircon as (a) showing a low-luminescent inherited magmatic core and a high-luminescent metamorphic rim, and a $^{207}Pb/^{206}Pb$ age; (c) zircon (PD-25b-02-31) contains inclusions of plagioclase, quartz and apatite in the inherited magmatic core and has no mineral inclusions in the rim; (d) CL image of the same zircon as (c) showing a low-luminescent inherited magmatic core and a high-luminescent metamorphic rim, and a $^{207}Pb/^{206}Pb$ age; (e) zircon (PD-25b-02-11) with no mineral inclusions; (f) CL image of the same metamorphic zircon as (e) showing a high-luminescent CL image, and a $^{207}Pb/^{206}Pb$ age; (g) zircon (PD-25b-02-7) with no mineral inclusions; (h) CL image of the same metamorphic zircon as (g) showing a middle-luminescent CL image, and a $^{207}Pb/^{206}Pb$ age.

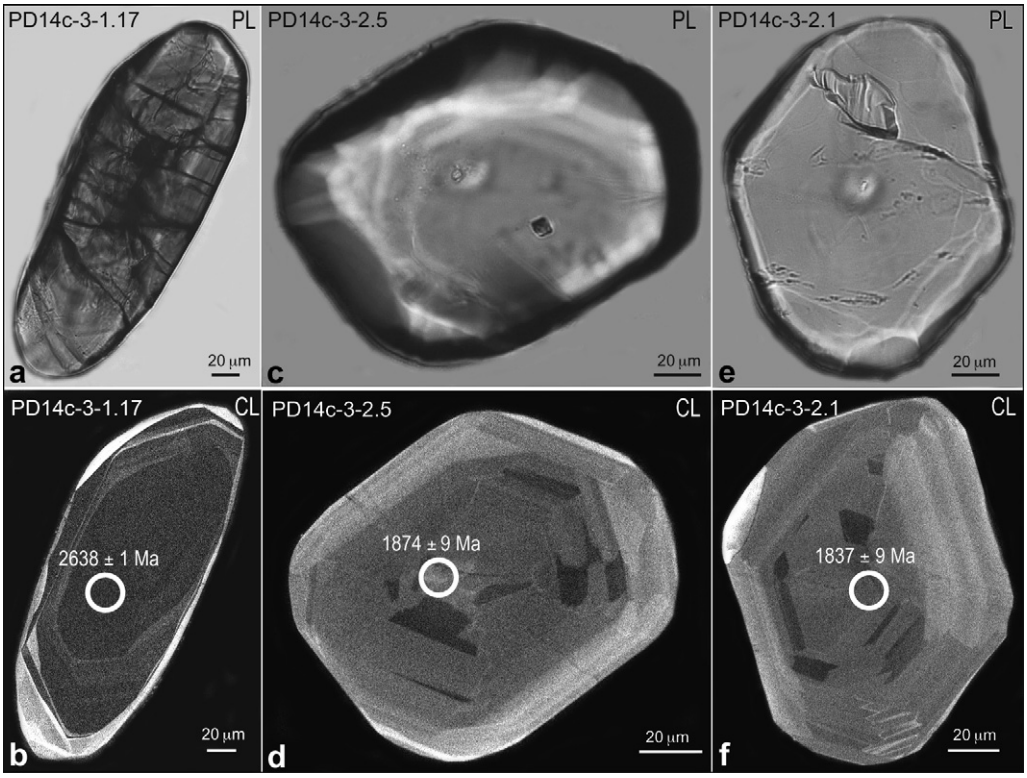

Figure 9 Plane-polarized light (PL) images of mineral inclusions, cathodoluminescence (CL) images and SIMS U-Pb ages of zircons from Px-bearing amphibolite (PD-14c-03). (a) Zircon (PD-14c-03-1.17) with no mineral inclusions; (b) CL image of the same zircon as (a) showing low-luminescent inherited core and high-luminescent metamorphic rim, and a $^{207}Pb/^{206}Pb$ age; (c) zircon PD-14c-03-2.5 with no mineral inclusions; (d) CL image of the same metamorphic zircon as (c) showing a high-luminescent CL image, and a $^{207}Pb/^{206}Pb$ age; (e) zircon (PD-14c-03-2.1) with no mineral inclusions; (f) CL image of the same metamorphic zircon as (e) showing a high-luminescent CL image, and a $^{207}Pb/^{206}Pb$ age.

(0.01–0.19) yielded apparent $^{207}Pb/^{206}Pb$ ages of (2511 ± 6)–(2195 ± 6) Ma, mainly concentrating from 2510 to 2450 Ma. The $^{207}Pb/^{206}Pb$ ages are similar to those recorded by metamorphic zircons in the TTG gneisses in the Qixia area, indicating a major metamorphic event at 2500–2400 Ma in the basement of Shandong Peninsula (Jahn et al., 2008). Seven spot analyses on metamorphic zircon domains with low Th/U ratios (0.13–0.73) yielded apparent $^{207}Pb/^{206}Pb$ ages of (1861 ± 9)–(1852 ± 6) Ma, consistent with the HP granulite facies metamorphic ages recorded by metamorphic zircon domains from PD-13d-02 (see below). Therefore, the $^{207}Pb/^{206}Pb$ ages represent the peak HP granulite facies metamorphism of Grt-Hy-granulite PD-16a-02. Twenty-two spot analyses on metamorphic zircon domains with Th/U ratios (0.08–0.66) yielded relatively younger apparent $^{207}Pb/^{206}Pb$ ages of (1849 ± 11)–(1825 ± 10) Ma, with a weighted mean age of 1839 ± 3 Ma (MSWD of 0.66; 17 spots) (Table 2; Fig. 10). These zircon domains contain Opx inclusions, indicating that the apparent $^{207}Pb/^{206}Pb$ ages may date medium to low-pressure granulite facies retrograde metamorphism.

6.2. Grt-amphibolite (PD-22a-28)

Although large age errors exist because of the low concentrations of U and Th in zircon from PD-22a-28, the $^{207}Pb/^{206}Pb$ ages (43 spot analyses) on different zircon grains can be subdivided into three groups (Table 3; Fig. 11).

Eleven spot analyses on inherited (magmatic) cores yielded consistent apparent $^{207}Pb/^{206}Pb$ ages clustering between 2604 ± 23 and 2510 ± 5 Ma (except for a few cores). This group of ages is consistent with a protolith age of 2535 ± 7 Ma for the TTG gneisses in the Qixia area (Zhou J.B. et al., 2008), and therefore represents the protolith age of Grt-amphibolite PD-22a-28. Six spot analyses of zircon domains yielded apparent $^{207}Pb/^{206}Pb$ ages of (2269 ± 121)–(1978 ± 67) Ma. These ages are generally older than the $^{206}Pb/^{238}U$ ages, and errors of both $^{207}Pb/^{206}Pb$ and $^{206}Pb/^{238}U$ ages are large (Table 3; Fig. 11), reflecting partial recrystallization and/or Pb loss. Eleven spot analyses of metamorphic zircon domains yielded consistent apparent $^{207}Pb/^{206}Pb$ ages of (1918 ± 37)–(1853 ± 12) Ma which are similar to HP granulite facies metamorphic ages of PD-16a-02 and PD-13d-02 (see below). Fifteen spot analyses on metamorphic zircon domains with low Th/U ratios (0.03–0.33) yielded the youngest apparent $^{207}Pb/^{206}Pb$ ages of (1849 ± 6)–(1748 ± 104) Ma with a weighted mean age of 1838 ± 5 Ma (MSWD of 2.10, 6 spots) (Table 3; Fig. 11). The zircon domains recording the youngest $^{207}Pb/^{206}Pb$ ages contain amphibole, representing retrograde metamorphism of Grt-amphibolite PD-22a-28.

6.3. Amp-two-Px-granulite (PD-13d-02 and PD-25b-02)

Zircons from sample PD-13d-02 record two groups of $^{207}Pb/^{206}Pb$ ages (Table 4; Fig. 12). Twenty-one spot analyses on metamorphic

Table 2 SIMS U-Pb analyses of zircons from retrograde HP granulite PD-16a-02.

Sample	Mineral inclusions	Contents (ppm)			Th/U	$^{207}Pb^*/^{206}Pb^*$	± (%)	$^{207}Pb^*/^{235}U$	± (%)	$^{206}Pb^*/^{238}U$	± (%)	Apparent age (Ma)	
		U	Th	$^{206}Pb^*$								$^{207}Pb^*/^{206}Pb^*$	$^{206}Pb^*/^{238}U$
$^{207}Pb/^{206}Pb$ ages of the first zircon domains: (2763 ± 5)–(2652 ± 8) Ma (5 spots)													
PD-16a-02.38	No	258	182	121	0.73	0.1924	0.3200	14.47	0.6200	0.5456	0.5300	2763 ± 5	2807 ± 12
PD-16a-02.41	No	372	595	178	1.65	0.1908	0.2700	14.60	0.6000	0.5548	0.5300	2749 ± 5	2845 ± 12
PD-16a-02.40	No	352	227	155	0.67	0.1905	0.4600	13.47	0.6500	0.5129	0.4700	2746 ± 8	2669 ± 10
PD-16a-02.39	No	206	183	89.8	0.92	0.1863	0.5300	13.05	0.8000	0.5079	0.6000	2710 ± 9	2648 ± 13
PD-16a-02.34	No	158	119	64.6	0.78	0.1799	0.4700	11.82	0.8400	0.4766	0.7000	2652 ± 8	2512 ± 15
$^{207}Pb/^{206}Pb$ ages of the second zircon domains: (2511 ± 6)–(2195 ± 6) Ma (9 spots)													
PD-16a-02.36	No	760	10.9	302	0.01	0.1654	0.3700	10.55	0.5100	0.4627	0.3500	2511 ± 6	2452 ± 7
PD-16a-02.30	No	2528	37.4	1020	0.02	0.1640	0.1200	10.63	0.2700	0.4701	0.2400	2497 ± 2	2484 ± 5
PD-16a-02.08	No	738	98.1	299	0.14	0.1632	0.3100	10.60	0.4800	0.4709	0.3600	2489 ± 5	2488 ± 8
PD-16a-02.18	No	365	47.2	144	0.13	0.1616	0.4000	10.21	0.8800	0.4583	0.7800	2472 ± 7	2432 ± 16
PD-16a-02.28	No	884	164	346	0.19	0.1613	0.2700	10.15	0.4200	0.4562	0.3300	2470 ± 5	2423 ± 7
PD-16a-02.19	No	552	72.3	219	0.14	0.1599	0.4600	10.18	0.6000	0.4615	0.4000	2455 ± 8	2446 ± 8
PD-16a-02.06	No	519	68.6	188	0.14	0.1550	1.8000	9.000	1.9000	0.4212	0.4700	2402 ± 31	2266 ± 9
PD-16a-02.22	No	2591	22.6	959	0.01	0.1505	0.6400	8.940	0.8000	0.4309	0.4700	2352 ± 11	2310 ± 9
PD-16a-02.05	No	558	72.6	184	0.13	0.1374	0.3400	7.261	0.5400	0.3833	0.4100	2195 ± 6	2092 ± 7
$^{207}Pb/^{206}Pb$ ages of the third zircon domains: (1861 ± 9)–(1852 ± 6) Ma (7 spots)													
PD-16a-02.07	No	288	36.2	80.9	0.13	0.1138	0.5100	5.133	0.7400	0.3272	0.5400	1861 ± 9	1825 ± 9
PD-16a-02.42	No	160	37.0	44.1	0.24	0.1137	0.6800	5.041	0.9700	0.3216	0.6900	1859 ± 12	1798 ± 11
PD-16a-02.31	No	150	36.9	41.2	0.26	0.1135	0.7400	5.013	1.5000	0.3204	1.3000	1856 ± 13	1792 ± 20
PD-16a-02.03	No	573	252	161	0.45	0.1133	0.4000	5.128	0.5700	0.3282	0.4100	1853 ± 7	1830 ± 7
PD-16a-02.02	No	157	45.1	44.5	0.30	0.1133	0.7800	5.161	1.1000	0.3303	0.8000	1853 ± 14	1840 ± 13
PD-16a-02.29	No	1221	863	334	0.73	0.1133	0.2500	4.980	0.3900	0.3188	0.3000	1853 ± 5	1784 ± 5
PD-16a-02.01	Qtz	847	437	236	0.53	0.1132	0.3200	5.060	0.5000	0.3241	0.3900	1852 ± 6	1810 ± 6
$^{207}Pb/^{206}Pb$ ages of the fourth zircon domains: (1839 ± 3) Ma (MSWD of 0.66, 17 spots, except for spots 26, 33, 32, 37 and 43)													
PD-16a-02.43	No	201	77.6	52.4	0.40	0.1130	0.6300	4.742	0.9000	0.3043	0.6300	1849 ± 11	1713 ± 10
PD-16a-02.10	No	132	33.4	37.4	0.26	0.1130	0.7500	5.157	1.1000	0.3311	0.7700	1848 ± 14	1844 ± 12
PD-16a-02.33	No	109	32.3	29.5	0.31	0.1129	0.9300	4.891	1.3000	0.3141	0.8500	1847 ± 17	1761 ± 13
PD-16a-02.21	No	336	138	93.6	0.43	0.1129	0.4700	5.049	0.6800	0.3243	0.4900	1847 ± 9	1811 ± 8
PD-16a-02.09	No	163	34.2	46.3	0.22	0.1129	0.7200	5.136	1.0000	0.3300	0.7000	1846 ± 13	1838 ± 11
PD-16a-02.13	No	647	413	181	0.66	0.1128	0.3500	5.062	0.5100	0.3255	0.3800	1845 ± 6	1816 ± 6
PD-16a-02.20	No	383	178	108	0.48	0.1128	0.4300	5.116	0.6400	0.3291	0.4700	1845 ± 8	1834 ± 8
PD-16a-02.17	No	1797	881	512	0.51	0.1127	0.2000	5.151	0.3400	0.3316	0.2700	1843 ± 4	1846 ± 4
PD-16a-02.04	No	546	227	153	0.43	0.1126	0.3800	5.064	0.5700	0.3262	0.4200	1841 ± 7	1820 ± 7
PD-16a-02.32	No	685	189	184	0.29	0.1125	0.3400	4.851	0.5100	0.3127	0.3700	1840 ± 6	1754 ± 6
PD-16a-02.16	No	771	248	216	0.33	0.1125	0.3100	5.061	0.4700	0.3263	0.3500	1840 ± 6	1821 ± 6
PD-16a-02.24	No	504	205	139	0.42	0.1125	0.3900	4.987	0.5800	0.3216	0.4200	1840 ± 7	1798 ± 7
PD-16a-02.25	No	1660	120.6	461	0.08	0.1124	0.2200	5.009	0.3500	0.3231	0.2700	1839 ± 4	1805 ± 4
PD-16a-02.11	Qtz	603	226	171	0.39	0.1124	0.3700	5.112	0.5400	0.3300	0.3900	1838 ± 7	1838 ± 6
PD-16a-02.26	No	154	50.7	41.7	0.34	0.1123	0.8000	4.886	1.1000	0.3156	0.7100	1837 ± 15	1768 ± 11
PD-16a-02.12	No	1121	403	314	0.37	0.1123	0.2600	5.051	0.4100	0.3263	0.3100	1837 ± 5	1820 ± 5
PD-16a-02.15	No	258	47.5	71.7	0.19	0.1122	0.5300	4.999	1.0000	0.3232	0.8500	1835 ± 10	1805 ± 13
PD-16a-02.37	No	524	238	138	0.47	0.1121	0.4000	4.726	0.5700	0.3057	0.4100	1834 ± 7	1720 ± 6
PD-16a-02.14	Amp	830	225	231	0.28	0.1121	0.3100	5.006	0.6700	0.3239	0.6000	1834 ± 6	1809 ± 9
PD-16a-02.23	No	133	33.0	36.9	0.26	0.1117	0.8800	4.961	1.2000	0.3221	0.7600	1828 ± 16	1800 ± 12
PD-16a-02.27	No	466	244	128	0.54	0.1117	0.4100	4.931	0.5900	0.3201	0.4300	1828 ± 7	1790 ± 7
PD-16a-02.35	No	264	141	72.2	0.55	0.1116	0.5700	4.890	0.8000	0.3179	0.5600	1825 ± 10	1779 ± 9

Pb* indicates radiogenic lead; Common Pb corrected using measured ^{204}Pb; all errors are 1 sigma.

Table 3 SIMS U-Pb analyses of zircons from retrograde HP granulite PD-22a-28.

Sample	Mineral inclusions	Contents (ppm)			Th/U	$^{207}Pb^*/^{206}Pb^*$	± (%)	$^{207}Pb^*/^{235}U$	± (%)	$^{206}Pb^*/^{238}U$	± (%)	Apparent age (Ma)	
		U	Th	$^{206}Pb^*$								$^{207}Pb^*/^{206}Pb^*$	$^{206}Pb^*/^{238}U$
$^{207}Pb/^{206}Pb$ ages of the first zircon domains: (2604 ± 23)~(2459 ± 68) Ma (11 spots)													
PD-22a-28.2	Ap + Qtz	51.2	35.4	35.9	0.69	0.1748	1.377	0.5148	1.563	12.4051	2.084	2604 ± 23	2677 ± 34
PD-22a-28.32	No	56.9	34.8	37.9	0.61	0.1746	0.561	0.4946	1.532	11.9085	1.631	2603 ± 9	2590 ± 33
PD-22a-28.3	Ap	172	137	118	0.79	0.1728	0.571	0.4918	1.509	11.7208	1.614	2585 ± 9	2579 ± 32
PD-22a-28.17	No	57.2	40.8	37.5	0.71	0.1727	1.186	0.4819	1.588	11.4765	1.982	2584 ± 20	2535 ± 33
PD-22a-28.30	Ap	49.6	27.8	34.3	0.56	0.1707	3.313	0.5142	1.507	12.1052	3.640	2565 ± 54	2675 ± 33
PD-22a-28.8	No	8.13	0.407	4.41	0.05	0.1687	2.668	0.4555	1.791	10.5936	3.213	2545 ± 44	2420 ± 36
PD-22a-28.15	Pl	94.8	15.3	54.0	0.16	0.1676	0.795	0.4715	1.520	10.8934	1.715	2533 ± 13	2490 ± 31
PD-22a-28.45	No	197	46.5	116	0.24	0.1652	0.308	0.4806	1.500	10.9489	1.531	2510 ± 5	2530 ± 31
PD-22a-28.37	No	602	636	408	1.06	0.1637	0.214	0.4668	1.504	10.5359	1.519	2494 ± 4	2470 ± 31
PD-22a-28.18	Cal	19.5	0.143	11.05	0.01	0.1635	1.679	0.4860	1.589	10.9546	2.312	2492 ± 28	2554 ± 34
PD-22a-28.33	No	1.72	0.066	–	0.04	0.1603	4.114	0.4745	1.712	10.4878	4.456	2459 ± 68	2503 ± 36
$^{207}Pb/^{206}Pb$ ages of the second zircon domains: (2269 ± 121)~(1978 ± 67) Ma (6 spots)													
PD-22a-28.16	No	1.73	0.743	0.731	0.43	0.1434	7.349	0.3274	1.680	6.4735	7.539	2269 ± 121	1826 ± 27
PD-22a-28.25	No	1.42	0.183	0.646	0.13	0.1399	4.348	0.3812	1.831	7.3534	4.718	2226 ± 73	2082 ± 33
PD-22a-28.23	No	5.80	0.949	2.56	0.16	0.1357	3.884	0.3690	1.515	6.9066	4.169	2174 ± 66	2025 ± 26
PD-22a-28.11	No	3.86	0.067	1.50	0.02	0.1234	4.957	0.3416	2.269	5.8093	5.452	2005 ± 85	1894 ± 37
PD-22a-28.39	Pl	1.82	0.204	0.699	0.11	0.1222	6.607	0.3358	1.678	5.6574	6.817	1988 ± 113	1867 ± 27
PD-22a-28.28	Pl + Grt	4.33	0.217	1.64	0.05	0.1215	3.840	0.3339	1.548	5.5926	4.140	1978 ± 67	1857 ± 25
$^{207}Pb/^{206}Pb$ ages of the third zircon domains: (1920 ± 92)~(1853 ± 45) Ma (11 spots)													
PD-22a-28.35	No	1.51	0.331	0.590	0.22	0.1176	5.277	0.3336	1.501	5.4102	5.486	1920 ± 92	1856 ± 24
PD-22a-28.40	No	18.8	1.15	6.93	0.06	0.1175	2.075	0.3271	1.514	5.2992	2.569	1918 ± 37	1825 ± 24
PD-22a-28.42	No	1.40	0.035	–	0.03	0.1156	7.175	0.3387	1.728	5.4008	7.380	1890 ± 124	1881 ± 28
PD-22a-28.47	No	2.03	0.484	0.806	0.24	0.1153	5.198	0.3345	2.771	5.3167	5.890	1884 ± 91	1860 ± 45
$^{207}Pb/^{206}Pb$ ages of the third zircon domains: (1920 ± 92)~(1853 ± 45) Ma (11 spots)													
PD-22a-28.1	No	8.40	0.370	–	0.04	0.1152	4.063	0.3261	1.610	5.1784	4.370	1883 ± 71	1819 ± 26
PD-22a-28.5	No	30.3	0.881	11.2	0.03	0.1150	2.310	0.3276	1.704	5.1954	2.871	1880 ± 41	1827 ± 27
PD-22a-28.13	No	1.72	0.224	–	0.13	0.1146	14.702	0.3991	2.094	6.3044	14.850	1873 ± 244	2165 ± 39
PD-22a-28.27	No	0.568	0.060	–	0.11	0.1140	12.066	0.3291	1.598	5.1735	12.172	1864 ± 203	1834 ± 26
PD-22a-28.41	No	2.37	0.047	0.864	0.02	0.1136	4.294	0.3253	1.629	5.0933	4.593	1857 ± 76	1815 ± 26
PD-22a-28.44	No	92.8	3.91	35.0	0.04	0.1133	0.665	0.3359	1.524	5.2487	1.662	1853 ± 12	1867 ± 25
PD-22a-28.43	No	6.74	0.530	2.64	0.08	0.1133	2.515	0.3456	1.555	5.3985	2.957	1853 ± 45	1913 ± 26
$^{207}Pb/^{206}Pb$ ages of the fourth zircon domains: (1838 ± 5) Ma (MSWD of 2.10, 6 spots, including spots 19, 20, 21, 29, 36 and 38)													
PD-22a-28.29	No	432	108	167	0.25	0.1131	0.320	0.3276	1.505	5.1072	1.539	1849 ± 6	1827 ± 24
PD-22a-28.38	No	601	139	235	0.23	0.1127	0.261	0.3308	1.507	5.1391	1.529	1843 ± 5	1842 ± 24
PD-22a-28.34	No	0.307	0.010	–	0.03	0.1127	30.004	0.4054	1.729	6.2969	30.054	1843 ± 462	2194 ± 32
PD-22a-28.31	No	5.41	0.219	2.17	0.04	0.1125	2.497	0.3570	1.503	5.5362	2.914	1840 ± 45	1968 ± 26
PD-22a-28.24	No	4.80	1.01	1.62	0.21	0.1124	3.913	0.2859	1.665	4.4298	4.252	1838 ± 69	1621 ± 24
PD-22a-28.36	No	757	129	294	0.17	0.1121	0.238	0.3349	1.501	5.1771	1.520	1834 ± 4	1862 ± 24
PD-22a-28.19	No	1294	409	520	0.32	0.1120	0.404	0.3343	1.501	5.1617	1.554	1832 ± 7	1859 ± 24
PD-22a-28.20	No	634	212	251	0.33	0.1118	0.426	0.3273	1.502	5.0471	1.561	1829 ± 8	1825 ± 24
PD-22a-28.26	No	3.58	0.393	1.40	0.11	0.1112	3.309	0.3407	1.617	5.2245	3.683	1820 ± 59	1890 ± 27
PD-22a-28.21	No	236	42.8	89.8	0.18	0.1110	0.733	0.3284	1.506	5.0283	1.675	1817 ± 13	1831 ± 24
PD-22a-28.10	Qtz	1.04	0.193	0.443	0.19	0.1102	13.295	0.3629	1.740	5.5156	13.408	1803 ± 224	1996 ± 30
PD-22a-28.7	No	14.5	0.828	–	0.06	0.1098	3.668	0.3300	1.576	4.9964	3.992	1796 ± 65	1839 ± 25
PD-22a-28.6	No	13.4	1.678	4.54	0.13	0.1096	3.833	0.2967	1.531	4.4827	4.128	1792 ± 68	1675 ± 23
PD-22a-28.22	No	0.221	0.044	–	0.20	0.1095	63.951	0.2571	9.360	3.8830	64.632	1792 ± 857	1475 ± 125
PD-22a-28.4	No	7.07	0.854	2.56	0.12	0.1069	5.893	0.3238	1.766	4.7742	6.152	1748 ± 104	1808 ± 28

Pb* indicates radiogenic lead; Common Pb corrected using measured ^{204}Pb; all errors are 1 sigma.

Table 4 SIMS U-Pb analyses of zircons from Amp-two-Px-granulite PD-13d-02.

Sample	Mineral inclusions	Contents (ppm)			Th/U	$^{207}Pb^*/^{206}Pb^*$	± (%)	$^{207}Pb^*/^{235}U$	± (%)	$^{206}Pb^*/^{238}U$	± (%)	Apparent age (Ma)	
		U	Th	$^{206}Pb^*$								$^{207}Pb^*/^{206}Pb^*$	$^{206}Pb^*/^{238}U$
$^{207}Pb/^{206}Pb$ ages of the first zircon domains: (1872 ± 12) Ma (MSWD of 0.52, 21 spots)													
PD-13d-02-28	Qtz + Grt	17.5	0.936	6.76	0.05	0.1180	1.548	5.6222	2.184	0.3457	1.540	1925 ± 27	1914 ± 26
PD-13d-02-1	No	17.9	0.320	6.51	0.02	0.1175	1.718	5.4101	2.317	0.3338	1.554	1919 ± 30	1857 ± 25
PD-13d-02-5	No	16.4	0.404	5.97	0.02	0.1163	1.798	5.3304	2.423	0.3324	1.623	1900 ± 32	1850 ± 26
PD-13d-02-10	No	21.9	1.41	8.06	0.06	0.1154	1.555	5.3122	2.188	0.3339	1.539	1886 ± 28	1857 ± 25
PD-13d-02-2	No	18.9	0.277	6.82	0.01	0.1152	1.671	5.2491	2.694	0.3305	2.112	1883 ± 30	1841 ± 34
PD-13d-02-17	Ap	28.8	0.845	10.5	0.03	0.1151	2.087	5.2838	2.587	0.3329	1.529	1882 ± 37	1852 ± 25
PD-13d-02-25	No	10.5	0.159	3.94	0.02	0.1150	2.080	5.4440	2.579	0.3434	1.524	1880 ± 37	1903 ± 25
PD-13d-02-22	Ap	30.3	0.580	11.3	0.02	0.1147	1.644	5.4167	2.245	0.3425	1.528	1875 ± 29	1899 ± 25
PD-13d-02-13	No	37.8	0.975	13.6	0.03	0.1146	1.182	5.1951	1.928	0.3288	1.523	1874 ± 21	1832 ± 24
PD-13d-02-14	No	47.1	4.57	17.1	0.10	0.1146	1.567	5.1785	2.182	0.3278	1.519	1873 ± 28	1828 ± 24
PD-13d-02-21	Ap	20.2	0.247	7.19	0.01	0.1145	2.299	5.1624	2.847	0.3270	1.679	1872 ± 41	1824 ± 27
PD-13d-02-4	No	27.3	0.464	9.95	0.02	0.1143	1.437	5.2815	2.180	0.3351	1.639	1869 ± 26	1863 ± 27
PD-13d-02-29	No	15.3	0.296	5.69	0.02	0.1141	2.638	5.3265	3.044	0.3386	1.518	1865 ± 47	1880 ± 25
PD-13d-02-20	Ap	19.1	0.150	–	0.01	0.1140	1.711	5.3155	2.304	0.3382	1.543	1864 ± 31	1878 ± 25
PD-13d-02-23	Ap	40.2	1.62	14.9	0.04	0.1139	1.117	5.3253	2.030	0.3392	1.695	1862 ± 20	1883 ± 28
PD-13d-02-27	No	23.1	0.302	8.55	0.01	0.1138	1.395	5.3124	2.157	0.3385	1.645	1862 ± 25	1879 ± 27
PD-13d-02-16	No	19.4	0.172	7.13	0.01	0.1138	1.604	5.2871	2.227	0.3371	1.545	1860 ± 29	1873 ± 25
PD-13d-02-12	No	48.4	1.96	17.7	0.04	0.1137	1.418	5.2218	2.069	0.3331	1.507	1859 ± 25	1854 ± 24
PD-13d-02-15	Ap	18.1	0.319	6.62	0.02	0.1136	2.102	5.2412	2.584	0.3346	1.502	1858 ± 37	1860 ± 24
PD-13d-02-30	Grt + Ap	58.4	2.97	21.6	0.05	0.1135	0.853	5.2543	1.728	0.3358	1.502	1856 ± 15	1866 ± 24
PD-13d-02-9	No	48.3	2.15	17.8	0.04	0.1133	1.169	5.2406	1.943	0.3354	1.551	1853 ± 21	1865 ± 25
$^{207}Pb/^{206}Pb$ ages of the second zircon domains: (1802 ± 31)∼(1846 ± 30) Ma (8 spots, except for spot 7)													
PD-13d-02-11	No	19.2	0.500	7.04	0.03	0.1129	1.701	5.2213	2.295	0.3355	1.542	1846 ± 30	1865 ± 25
PD-13d-02-6	Rt + Pl	15.6	1.28	5.81	0.08	0.1125	1.811	5.2272	2.355	0.3370	1.505	1840 ± 32	1872 ± 24
PD-13d-02-18	No	21.4	0.472	7.85	0.02	0.1123	2.351	5.1995	2.850	0.3358	1.611	1837 ± 42	1867 ± 26
$^{207}Pb/^{206}Pb$ ages of the second zircon domains: 1802 ± 31∼1846 ± 30 Ma (8 spots, except for spot 7)													
PD-13d-02-26	No	41.7	2.26	15.3	0.05	0.1120	1.149	5.1410	1.905	0.3330	1.519	1832 ± 21	1853 ± 25
PD-13d-02-3	Ap	24.0	0.582	8.74	0.02	0.1119	1.484	5.1442	2.137	0.3333	1.537	1831 ± 27	1854 ± 25
PD-13d-02-19	Grt + Ap	47.6	5.25	17.6	0.11	0.1110	1.088	5.1073	1.867	0.3338	1.518	1815 ± 20	1857 ± 25
PD-13d-02-24	Ap	18.0	0.208	6.54	0.01	0.1105	1.646	5.0805	2.434	0.3333	1.793	1808 ± 30	1854 ± 29
PD-13d-02-8	Grt	17.6	0.206	6.37	0.01	0.1102	1.705	5.0512	2.302	0.3326	1.547	1802 ± 31	1851 ± 25
PD-13d-02-7	Ap	13.3	0.674	4.84	0.05	0.1090	2.585	5.0415	3.020	0.3354	1.562	1783 ± 46	1865 ± 25

Pb* indicates radiogenic lead; Common Pb corrected using measured ^{204}Pb; all errors are 1 sigma.

zircons with low Th/U ratios (0.01–0.10) and HP granulite facies mineral inclusions, yielded consistent apparent $^{207}Pb/^{206}Pb$ ages of (1925 ± 27)–(1853 ± 21) Ma with a weighted mean of 1872 ± 12 Ma (MSWD of 0.52; 21 spots), which represent the peak HP granulite facies metamorphic ages. In contrast, 9 spot analyses on metamorphic zircon domains with no mineral inclusions yielded younger consistent apparent $^{207}Pb/^{206}Pb$ ages ranging from 1846 ± 30 to 1802 ± 31 Ma (except for one spot) (Table 4; Fig. 11), which are considered to represent retrograde metamorphic ages.

The $^{207}Pb/^{206}Pb$ ages recorded in different zircon domains of PD-25b-02 are relatively complex, and subdivided into four groups (Table 5; Fig. 13). Five analyzed spots on inherited (magmatic) cores with low Th/U ratios (0.21–0.44) yielded consistent apparent $^{207}Pb/^{206}Pb$ ages of (2915 ± 7)–(2890 ± 9) Ma, which might represent the protolith age of Amp-two-Px-granulite PD-25b-02. Some TTG gneisses in the study area record similar protolith ages of ∼2900 Ma (Jahn et al., 2008), indicating a magmatic event in the Early Precambrian metamorphic basement of the Shandong Peninsula at this time. In contrast, eight inherited (magmatic) cores with mineral inclusions of Pl + Qtz + Ap + Bt + Ep + Orp yielded younger $^{207}Pb/^{206}Pb$ ages of (2198 ± 13)–(2141 ± 14) Ma, indicating that these zircons may be contaminated grains. However, fourteen spot analyses on metamorphic zircon domains are characterized by extremely low Th/U ratios (0.01–0.11), and yielded $^{207}Pb/^{206}Pb$ ages of (1928 ± 57)–(1852 ± 18) Ma with a weighted mean age of 1871 ± 8 Ma (MSWD of 0.53, 11 spots). These ages are inferred to indicate the timing of HP granulite facies metamorphism. In addition, nine analyzed spots on metamorphic zircon domains with low Th/U ratios (0.02–0.16) yielded the youngest $^{207}Pb/^{206}Pb$ ages of (1840 ± 27)–(1822 ± 19) Ma, consistent with those recorded by Opx-bearing zircon domains in sample PD-16a-02, and represents medium to low-pressure granulite facies retrograde metamorphic ages.

6.4. Px-bearing amphibolite (PD-14c-03)

The $^{207}Pb/^{206}Pb$ ages recorded in different zircon domains from PD-14c-03 can be subdivided into three groups (Table 6; Fig. 14).

Table 5 SIMS U-Pb analyses of zircons from Amp-Two-Px-granulite PD-25b-02.

Sample	Mineral inclusions	Contents (ppm)			Th/U	$^{207}Pb^*/^{206}Pb^*$	±1σ	$^{207}Pb^*/^{235}U$	±1σ	$^{206}Pb^*/^{238}U$	±1σ	Apparent age (Ma)	
		U	Th	$^{206}Pb^*$								$^{207}Pb^*/^{206}Pb^*$	$^{206}Pb^*/^{238}U$
$^{207}Pb/^{206}Pb$ ages of the first zircon domains: (2915 ± 7)~(2890 ± 9) Ma (4 spots, except for spot 2)													
PD-25b-02.5	Ap	223	62.2	160	0.28	0.21121	0.4432	16.3030	1.593	0.5598	1.530	2915 ± 7	2866 ± 36
PD-25b-02.15	Ap	351	75.0	257	0.21	0.21063	0.1688	16.6900	1.509	0.5747	1.500	2910 ± 3	2927 ± 35
PD-25b-02.25	No	167	63.8	123	0.38	0.20992	0.2555	16.1434	1.554	0.5578	1.533	2905 ± 4	2857 ± 35
PD-25b-02.29	Ap	62.5	27.6	46.0	0.44	0.20800	0.5649	15.9186	1.644	0.5551	1.544	2890 ± 9	2846 ± 36
PD-25b-02.2	Ap	382	110	247	0.29	0.19510	0.3634	13.6589	1.546	0.5078	1.503	2786 ± 6	2647 ± 33
$^{207}Pb/^{206}Pb$ ages of the second zircon domains: (2182 ± 12) Ma (MSWD of 0.60, 6 spots, except for spots 24 and 36)													
PD-25b-02.35	Qtz + Pl + Bt + Ap	56.3	44.6	30.9	0.79	0.13765	0.7256	7.7229	1.668	0.4069	1.502	2198 ± 13	2201 ± 28
PD-25b-02.10	Ap	67.2	65.4	37.6	0.97	0.13672	1.2593	7.5507	2.180	0.4005	1.779	2186 ± 22	2171 ± 33
PD-25b-02.19	Ap	50.1	34.7	26.9	0.69	0.13666	0.7603	7.5603	1.694	0.4012	1.514	2185 ± 13	2175 ± 28
PD-25b-02.30	Ap	65.4	54.1	36.1	0.83	0.13629	0.8951	7.5676	1.747	0.4027	1.500	2181 ± 15	2182 ± 28
PD-25b-02.31	Qtz + Pl + Ap	72.6	58.8	39.0	0.81	0.13567	0.6514	7.4166	1.744	0.3965	1.618	2173 ± 11	2153 ± 30
PD-25b-02.21	Qtz + Pl + Ap + Cal	40.2	23.6	21.3	0.59	0.13535	1.0081	7.5797	1.812	0.4061	1.506	2169 ± 17	2197 ± 28
PD-25b-02.36	Ap	45.9	25.0	23.2	0.54	0.13342	0.8518	7.2476	1.840	0.3940	1.630	2144 ± 15	2141 ± 30
PD-25b-02.24	Qtz + Ap + Orp	64.6	46.2	34.1	0.72	0.13321	0.7772	7.2095	1.697	0.3925	1.509	2141 ± 14	2135 ± 27
$^{207}Pb/^{206}Pb$ ages of the third zircon domains (1871 ± 8) Ma (MSWD of 0.53, 11 spots, except for spots 4, 11 and 17)													
PD-25b-02.4	No	20.0	2.24	7.52	0.11	0.11813	3.2255	5.3485	3.739	0.3284	1.892	1928 ± 57	1831 ± 30
PD-25b-02.11	No	20.0	0.184	7.59	0.01	0.11729	2.3779	5.4800	2.856	0.3388	1.581	1915 ± 42	1881 ± 26
PD-25b-02.16	No	31.3	0.295	11.4	0.01	0.11562	0.8758	5.1917	1.747	0.3257	1.512	1890 ± 16	1817 ± 24
PD-25b-02.34	No	30.0	0.766	11.2	0.03	0.11527	1.3560	5.2809	2.093	0.3323	1.594	1884 ± 24	1849 ± 26
PD-25b-02.13	No	77.4	1.01	28.3	0.01	0.11495	0.6067	5.1872	1.623	0.3273	1.505	1879 ± 11	1825 ± 24
PD-25b-02.32	No	32.5	1.06	12.2	0.03	0.11481	1.1306	5.2717	1.903	0.3330	1.531	1877 ± 20	1853 ± 25
PD-25b-02.18	No	75.8	1.30	28.4	0.02	0.11457	0.6397	5.2768	1.638	0.3341	1.508	1873 ± 11	1858 ± 24
PD-25b-02.22	No	140	3.87	52.6	0.03	0.11453	0.4545	5.2813	1.571	0.3344	1.504	1873 ± 8	1860 ± 24
PD-25b-02.8	No	81.5	2.83	30.7	0.03	0.11443	1.2256	5.2912	1.954	0.3354	1.522	1871 ± 22	1864 ± 25
$^{207}Pb/^{206}Pb$ ages of the third zircon domains (1871 ± 8) Ma (MSWD of 0.53, 11 spots, except for spots 4, 11 and 17)													
PD-25b-02.27	No	87.6	1.26	32.8	0.01	0.11430	0.7398	5.2815	1.673	0.3351	1.501	1869 ± 13	1863 ± 24
PD-25b-02.20	No	18.3	0.429	6.81	0.02	0.11363	1.3305	5.2080	2.051	0.3324	1.561	1858 ± 24	1850 ± 25
PD-25b-02.14	No	66.3	2.13	24.9	0.03	0.11355	0.7205	5.2248	1.670	0.3337	1.507	1857 ± 13	1856 ± 24
PD-25b-02.23	No	107	2.63	39.7	0.02	0.11343	0.7416	5.1936	1.678	0.3321	1.505	1855 ± 13	1848 ± 24
PD-25b-02.17	No	24.6	1.05	8.92	0.04	0.11322	0.9943	5.0286	1.829	0.3221	1.536	1852 ± 18	1800 ± 24
$^{207}Pb/^{206}Pb$ ages of the fourth zircon domains (1840 ± 27)~(1822 ± 19) Ma (7 spots, except for spots 6 and 33)													
PD-25b-02.6	No	4.79	0.087	–	0.02	0.11247	8.5371	4.9923	8.668	0.3219	1.500	1840 ± 147	1799 ± 24
PD-25b-02.12	No	91.0	14.2	33.8	0.16	0.11246	1.4869	4.9973	2.131	0.3223	1.526	1840 ± 27	1801 ± 24
PD-25b-02.1	No	306	15.2	114	0.05	0.11235	0.6419	5.1233	1.638	0.3307	1.507	1838 ± 12	1842 ± 24
PD-25b-02.28	No	67.1	1.39	24.8	0.02	0.11232	0.7200	5.1075	1.688	0.3298	1.527	1837 ± 13	1837 ± 24
PD-25b-02.3	No	45.9	1.36	17.4	0.03	0.11230	1.9262	5.2355	2.654	0.3381	1.825	1837 ± 34	1878 ± 30
PD-25b-02.9	No	87.6	1.63	32.8	0.02	0.11170	1.1801	5.1620	1.914	0.3352	1.507	1827 ± 21	1863 ± 24
PD-25b-02.26	No	6.99	0.116	2.69	0.02	0.11145	3.2258	5.2857	3.584	0.3440	1.561	1823 ± 57	1906 ± 26
PD-25b-02.7	No	123	3.09	45.6	0.03	0.11140	1.0358	5.1080	1.832	0.3326	1.511	1822 ± 19	1851 ± 24
PD-25b-02.33	No	2.78	0.079	1.06	0.03	0.10546	4.0601	4.9664	4.331	0.3415	1.507	1722 ± 73	1894 ± 25

Pb* indicates radiogenic lead; Common Pb corrected using measured ^{204}Pb; all errors are 1 sigma.

Table 6 SIMS U-Pb analyses of zircon from Px-bearing amphibolite PD-14c-03.

Sample	Mineral inclusions	Contents (ppm)			Th/U	$^{207}Pb^*/^{206}Pb^*$	± (%)	$^{207}Pb^*/^{235}U$	± (%)	$^{206}Pb^*/^{238}U$	± (%)	Apparent age (Ma)	
		U	Th	$^{206}Pb^*$								$^{207}Pb^*/^{206}Pb^*$	$^{206}Pb^*/^{238}U$
$^{207}Pb/^{206}Pb$ ages of the first zircon domains: (2656 ± 3)~(2595 ± 3) Ma (11 spots)													
PD-14C-03-1.7	No	1576	182	965	0.12	0.1803	0.2024	12.888	1.514	0.5184	1.501	2656 ± 3	2692 ± 33
PD-14C-03-1.5	Pl + Ap	2014	163	1247	0.08	0.1798	0.2512	13.010	1.534	0.5249	1.513	2651 ± 4	2720 ± 34
PD-14C-03-1.6	No	1870	162	1138	0.09	0.1795	0.4034	12.773	1.558	0.5162	1.505	2648 ± 7	2683 ± 33
PD-14C-03-1.14	No	1461	111	873	0.08	0.1785	0.3226	12.553	1.538	0.5101	1.504	2639 ± 5	2657 ± 33
PD-14C-03-1.17	No	2794	210	1694	0.08	0.1784	0.0838	12.755	1.502	0.5186	1.500	2638 ± 1	2693 ± 33
PD-14C-03-1.16	No	4017	316	2440	0.08	0.1775	0.3277	12.741	1.540	0.5207	1.505	2629 ± 5	2702 ± 33
PD-14C-03-1.1	Qtz	2233	167	1396	0.07	0.1775	0.5057	12.833	1.587	0.5245	1.505	2629 ± 8	2718 ± 33
PD-14C-03-1.20	No	2927	224	1742	0.08	0.1772	0.0877	12.558	1.503	0.5140	1.500	2627 ± 1	2673 ± 33
PD-14C-03-1.9	No	1104	89.0	649	0.08	0.1764	0.4629	12.249	1.571	0.5037	1.501	2619 ± 8	2630 ± 33
PD-14C-03-1.13	Pl	2625	250	1562	0.10	0.1743	0.4334	12.221	1.566	0.5086	1.504	2599 ± 7	2651 ± 33
PD-14C-03-1.10	Qtz	1930	237	1139	0.12	0.1738	0.2034	12.041	1.514	0.5024	1.501	2595 ± 3	2624 ± 32
$^{207}Pb/^{206}Pb$ ages of the second zircon domains: 1923 ± 75~2495 ± 16 Ma (6 spots)													
PD-14C-03-2.3	No	30.5	0.274	16.9	0.01	0.1638	0.9669	10.973	1.817	0.4858	1.538	2495 ± 16	2553 ± 32
PD-14C-03-2.6	No	100	0.753	53.1	0.01	0.1628	0.6082	10.522	1.671	0.4686	1.556	2485 ± 10	2478 ± 32
PD-14C-03-1.12	Ap	46.9	0.079	21.9	0.00	0.1436	1.486	8.2344	2.124	0.4158	1.518	2271 ± 25	2242 ± 29
PD-14C-03-2.9	No	4.44	0.559	1.99	0.13	0.1411	6.744	7.6949	6.938	0.3954	1.628	2241 ± 112	2148 ± 30
PD-14C-03-2.7	No	4.05	0.221	1.52	0.05	0.1228	3.609	5.7020	4.025	0.3368	1.782	1997 ± 63	1871 ± 29
PD-14C-03-2.10	No	4.20	0.084	–	0.02	0.1178	4.315	5.5640	4.677	0.3426	1.804	1923 ± 75	1899 ± 30
$^{207}Pb/^{206}Pb$ ages of the third zircon domains: (1866 ± 11) Ma (MSWD of 2.2, 9 spots, except for spot 1.18)													
PD-14C-03-1.3	Qtz	116	2.24	44.3	0.02	0.1159	0.5344	5.4946	1.597	0.3439	1.504	1894 ± 10	1905 ± 25
PD-14C-03-1.8	Qtz	82	2.27	30.5	0.03	0.1156	0.7303	5.3966	1.676	0.3386	1.509	1889 ± 13	1880 ± 25
PD-14C-03-2.5	Ap + Qtz	197	5.14	71.7	0.03	0.1146	0.5104	5.2842	1.586	0.3344	1.502	1874 ± 9	1860 ± 24
PD-14C-03-1.2	No	209	5.62	79.3	0.03	0.1143	0.6370	5.3800	1.630	0.3414	1.500	1869 ± 11	1893 ± 25
PD-14C-03-1.4	No	144	4.01	53.4	0.03	0.1136	0.5034	5.2480	1.604	0.3351	1.523	1857 ± 9	1863 ± 25
$^{207}Pb/^{206}Pb$ ages of the third zircon domains: (1866 ± 11) Ma (MSWD of 2.2, 9 spots, except for spot 1.18)													
PD-14C-03-1.15	No	390	8.67	145	0.02	0.1136	0.3611	5.2884	1.545	0.3377	1.502	1857 ± 7	1876 ± 24
PD-14C-03-2.4	No	188	7.29	68.2	0.04	0.1136	0.5719	5.1936	1.609	0.3317	1.504	1857 ± 10	1847 ± 24
PD-14C-03-1.18	No	177	7.19	63.0	0.04	0.1134	0.5450	5.0643	1.600	0.3240	1.504	1854 ± 10	1809 ± 24
PD-14C-03-1.11	No	177	4.55	65.7	0.03	0.1133	1.105	5.2911	1.867	0.3386	1.505	1853 ± 20	1880 ± 25
PD-14C-03-1.19	No	305	4.16	113	0.01	0.1133	0.5394	5.2768	1.617	0.3377	1.524	1853 ± 10	1876 ± 25
$^{207}Pb/^{206}Pb$ ages of the fourth zircon domains: (1837 ± 9)~(1825 ± 12) Ma (2 spots)													
PD-14C-03-2.1	No	187	10.1	70.1	0.05	0.1123	0.5056	5.2767	1.590	0.3407	1.507	1837 ± 9	1890 ± 25
PD-14C-03-2.2	No	159	5.52	57.5	0.03	0.1116	0.6842	5.1157	1.651	0.3326	1.502	1825 ± 12	1851 ± 24

Pb* indicates radiogenic lead; Common Pb corrected using measured ^{204}Pb; all errors are 1 sigma.

Eleven spot analyses on inherited (magmatic) cores with mineral inclusions of Cpx + Pl + Qtz yielded $^{207}Pb/^{206}Pb$ ages of (2656 ± 3)–(2595 ± 3) Ma, corresponding to protolith ages. However, some magmatic zircon cores record younger $^{207}Pb/^{206}Pb$ ages ranging from 2495 ± 16 to 1923 ± 75 Ma, indicating that they have experienced partial recrystallization and Pb loss related to later metamorphic events. Ten spot analyses on metamorphic zircon domains are characterized by low Th/U ratios (0.01–0.04) and Grt + Cpx + Pl + Qtz mineral inclusions, and yielded consistent HP granulite facies metamorphic ages of (1894 ± 10)–(1853 ± 10) Ma with a weighted mean age of 1866 ± 11 Ma (MSWD of 2.20; 9 spots). Two spot analyses on metamorphic zircon domains yielded youngest $^{207}Pb/^{206}Pb$ ages of 1825 ± 12 Ma and 1837 ± 9 Ma, which are similar to the ages recorded by Opx-bearing zircon domains in sample PD-16a-02, and represents the timing of medium to low-pressure granulite facies retrograde recrystallization.

7. Discussion and conclusions

7.1. Implications of mineral inclusions in zircon from HP granulites

Although substantial progress has been made in elucidating the petrology, mineralogy, metamorphism and geochronology of the HP granulites in the Early Precambrian metamorphic basement of the NCC in the past 20 years (Wang et al., 1991; Zhai et al., 1992, 1994; Guo et al., 1993, 1998, 2002, 2005; Geng and Ji, 1994; Ma and Wang, 1995; Li et al., 1997; Liu et al., 1998, 2002, 2010, 2011; Wei et al., 2001; Zhao, 2001, 2009; Zhao et al., 2001, 2003, 2005, 2009, 2010, 2011; Zhou X.W. et al., 2003, 2004, 2007, 2008, 2010; Zhai, 2004, 2009; Kröner et al., 2005, 2006; O'Brien et al., 2005; Wan et al., 2006, 2010; Zhang H.F. et al., 2006; Li and Zhao, 2007; Tang et al., 2007;

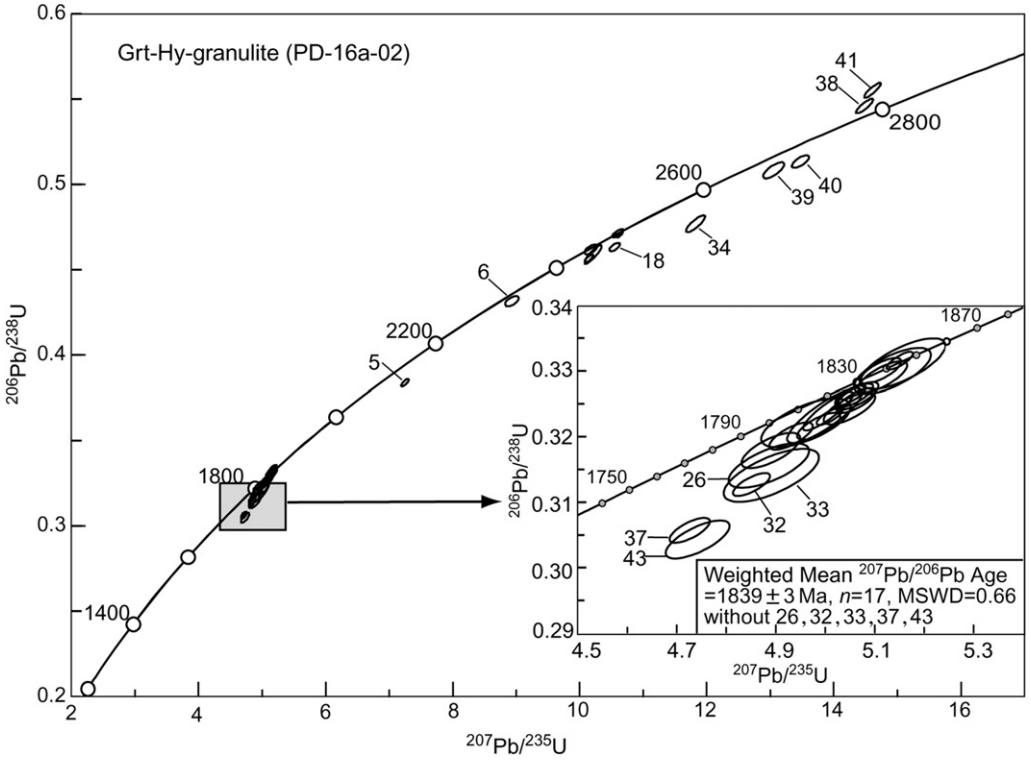

Figure 10 Zircon U-Pb concordia diagram ($^{207}Pb/^{235}U$ - $^{206}Pb/^{238}U$) of Grt-Hy-granulite PD-16a-02.

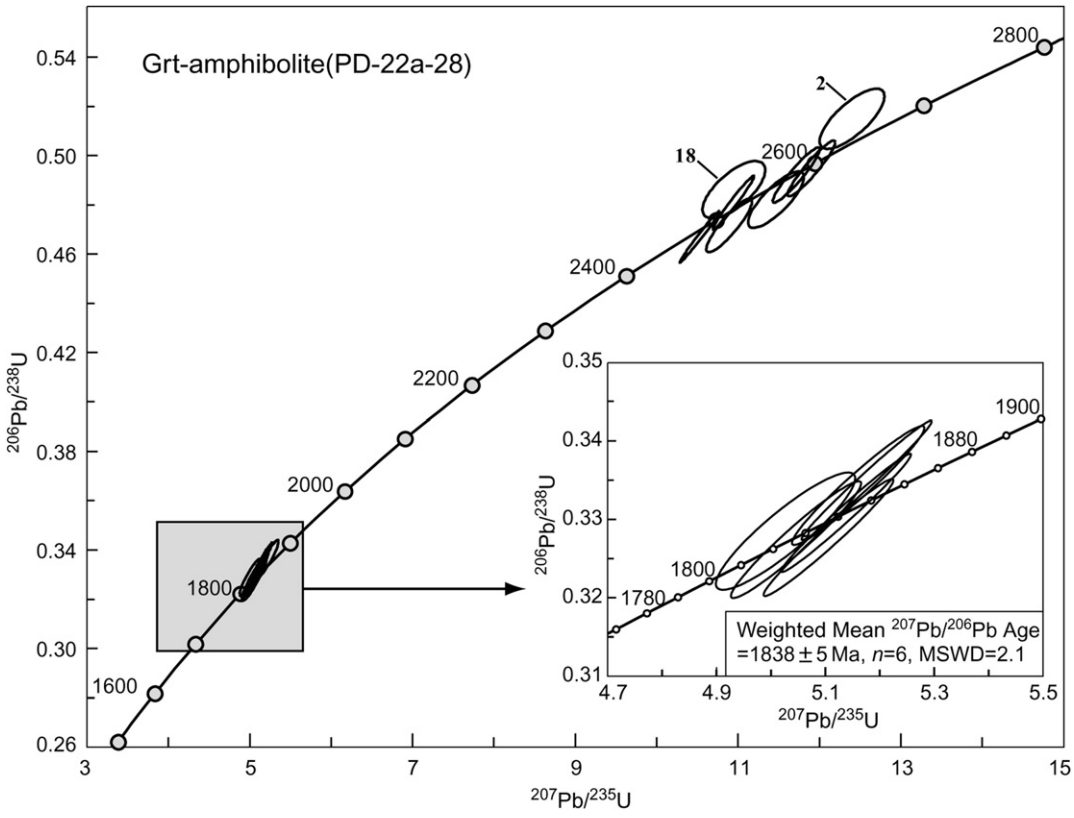

Figure 11 Zircon U-Pb concordia diagram ($^{207}Pb/^{235}U$ - $^{206}Pb/^{238}U$) of Grt-amphibolite PD-22a-28.

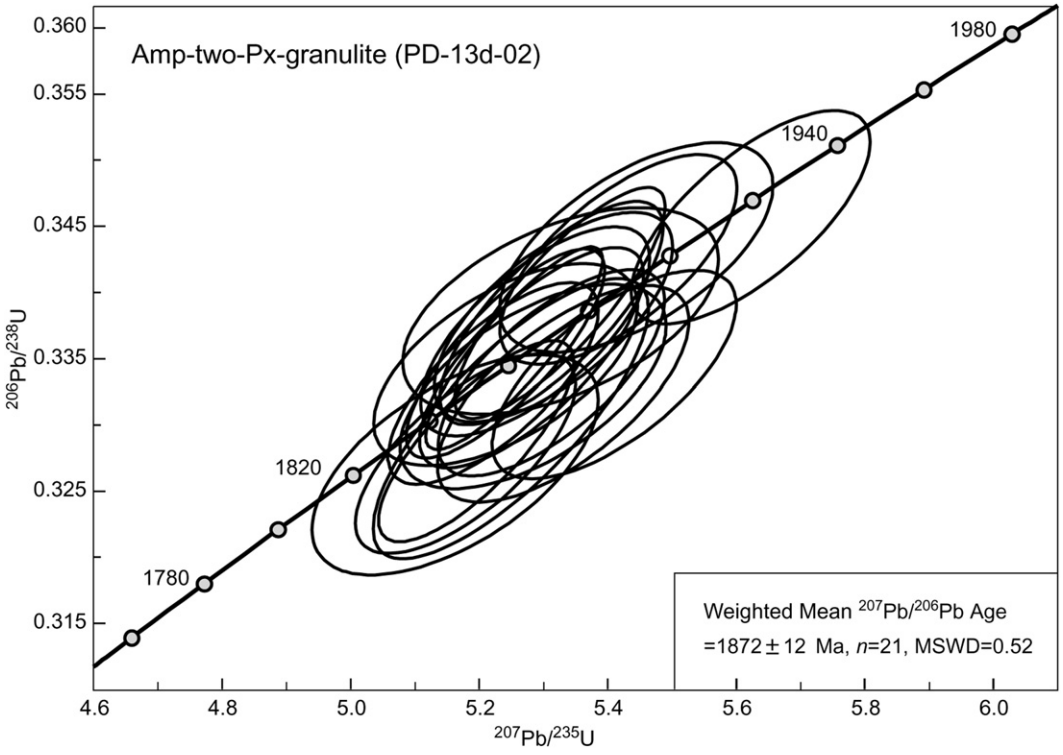

Figure 12 Zircon U-Pb concordia diagram ($^{207}Pb/^{235}U$ - $^{206}Pb/^{238}U$) of Amp-two-Px-granulite PD-13d-02.

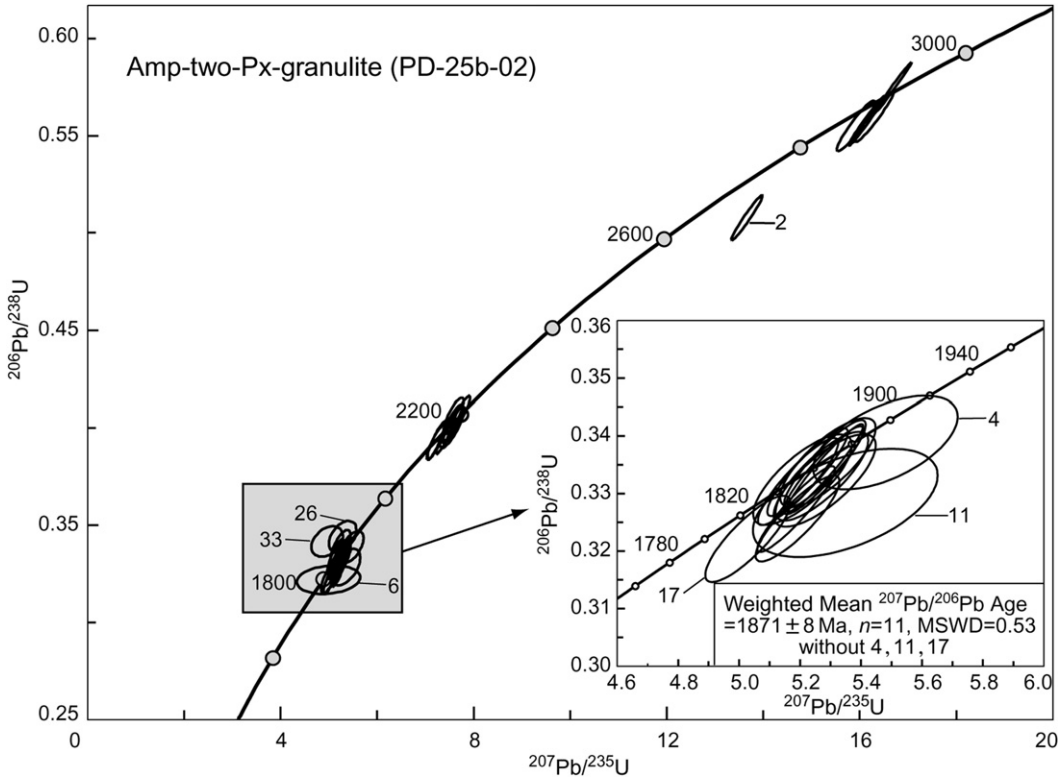

Figure 13 Zircon U-Pb concordia diagram ($^{207}Pb/^{235}U$ - $^{206}Pb/^{238}U$) of Amp-two-Px-granulite PD-25b-02.

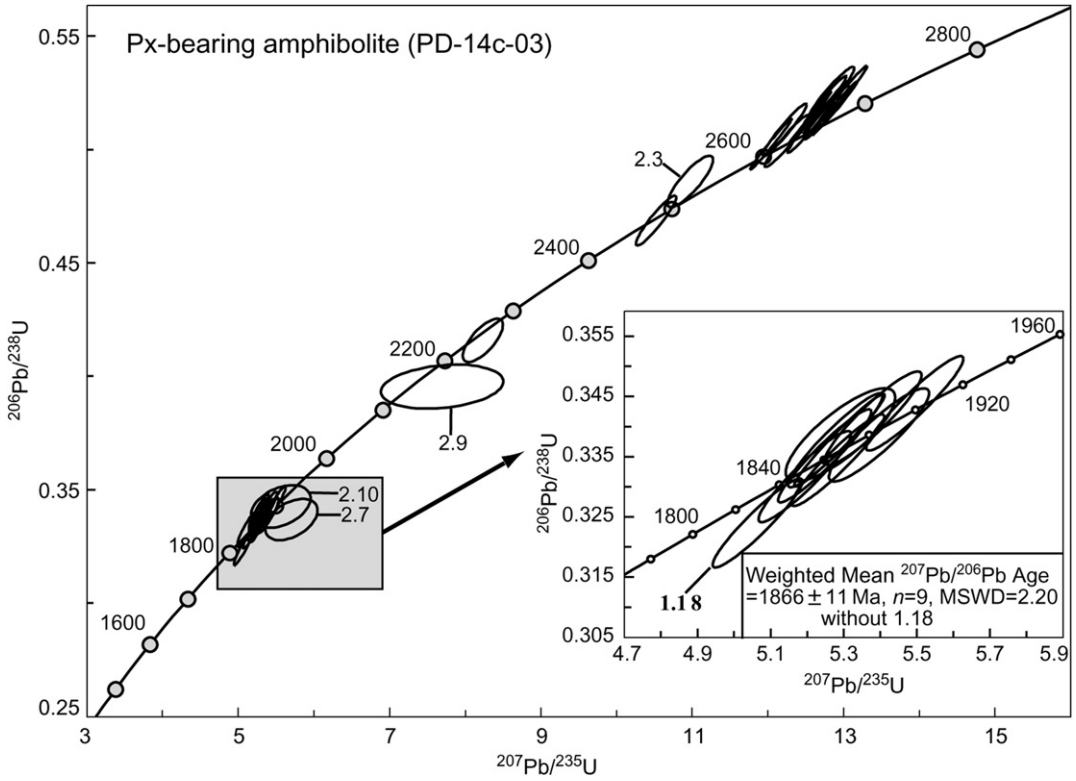

Figure 14 Zircon U-Pb concordia diagram ($^{207}Pb/^{235}U$ - $^{206}Pb/^{238}U$) of Px-bearing amphibolite PD-14c-03.

Jahn et al., 2008; Luo et al., 2008; Zhou J.B. et al., 2008; Guo and Li, 2009; Wang et al., 2009; Yin et al., 2009, 2011; Tam et al., 2011, 2012, Zhai and Santosh, 2011), detailed studies on zircons, especially their mineral inclusions, are lacking. Our study recorded the occurrence of mineral inclusion assemblages of Grt + Cpx + Pl + Qtz + Rt + Ap in the metamorphic zircon domains from the HP granulites represented by the widely distributed Amp-two-Px-granulites and (Px-bearing) amphibolites in the Early Precambrian metamorphic basement of Shandong Peninsula (Fig. 15).

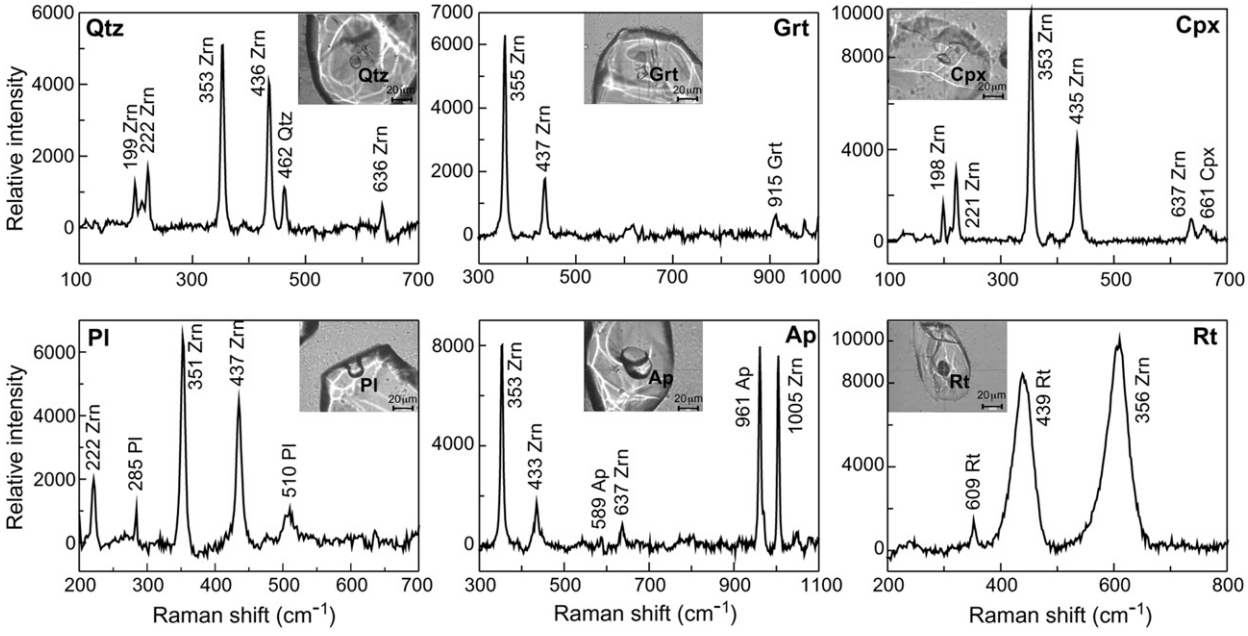

Figure 15 Representative Raman spectra of mineral inclusions in zircons from the Amp-two-Px-granulites (PD-13d-02).

Table 7 U-Pb ages of zircons from the HP granulites and country rocks, Shandong Peninsula.

Sample Nos.	Locality	Rock type	Metamorphic ages (Ma)	References	Analytical methods
03SD-06	Qixia	Amphibolite	1769 ± 60	Tang et al. (2007)	LA-ICP-MS
02SD-33	Qixia	Mafic granulite	1794 ± 41		
S0141-1	Yantai	Two-Mic-Sil-Grt-paragneiss	1882 ± 12	Wan et al. (2006)	SHRIMP
S0116-1	Yantai	Grt-Mus-Qtz-schist	1850–1900		
SD6	Qixia	Amphibolite	1865 ± 3	Zhou J.B. et al. (2008)	
LY-6	Qixia	Pelitic HP granulite	1846 ± 9	Zhou X.W. et al. (2008)	
08JB06-4	Laixi	Grt-pyroxenite	1956 ± 41	Tam et al. (2011)	SHRIMP
08JB06-1-6	Pingdu	Mafic HP granulite	1884 ± 42		
08JB07-1	Qixia	Pelitic HP granulite	1837 ± 8		
08JB02-1	Laixi	Grt-Sil-paragneiss	1939 ± 15		
			1821 ± 8		
08JB03-1	Laixi	Grt-Cord-Bt-paragneiss	1836 ± 68		
08JB05-1	Laixi	Cpx-mables	1817 ± 9		
08JB02-10	Laixi	Qtz-bearing mables	1790 ± 6		

7.2. Protolith ages

Only part of the inherited (magmatic) cores from five samples contains minor mineral inclusions such as apatite. U-Pb zircon ages indicate several protolith ages of the HP granulites in the Shandong Peninsula. The $^{207}Pb/^{206}Pb$ ages concentrated between 2915–2890 Ma and 2763–2510 Ma are taken to represent protolith ages of the HP granulites. These ages are consistent with zircon ages in the TTG gneisses of the study area (Tang et al., 2007; Jahn et al., 2008; Zhou J.B. et al., 2008; Liu et al., 2011). They also indicate that widespread magmatic events occurred in the metamorphic basement of the southeastern boundary of the NCC in the Late Mesoarchean and Late Neoarchean.

However, it should be noted that a group of inherited (magmatic) zircon cores from the Amp-two-Px-granulite PD-25b-02 record a Palaeoproterozoic growth event (2198 ± 13)–(2141 ± 14) Ma. The main mineral inclusions in these zircon cores are Pl + Qtz + Ap + Bt + Ep + Qrp, which are

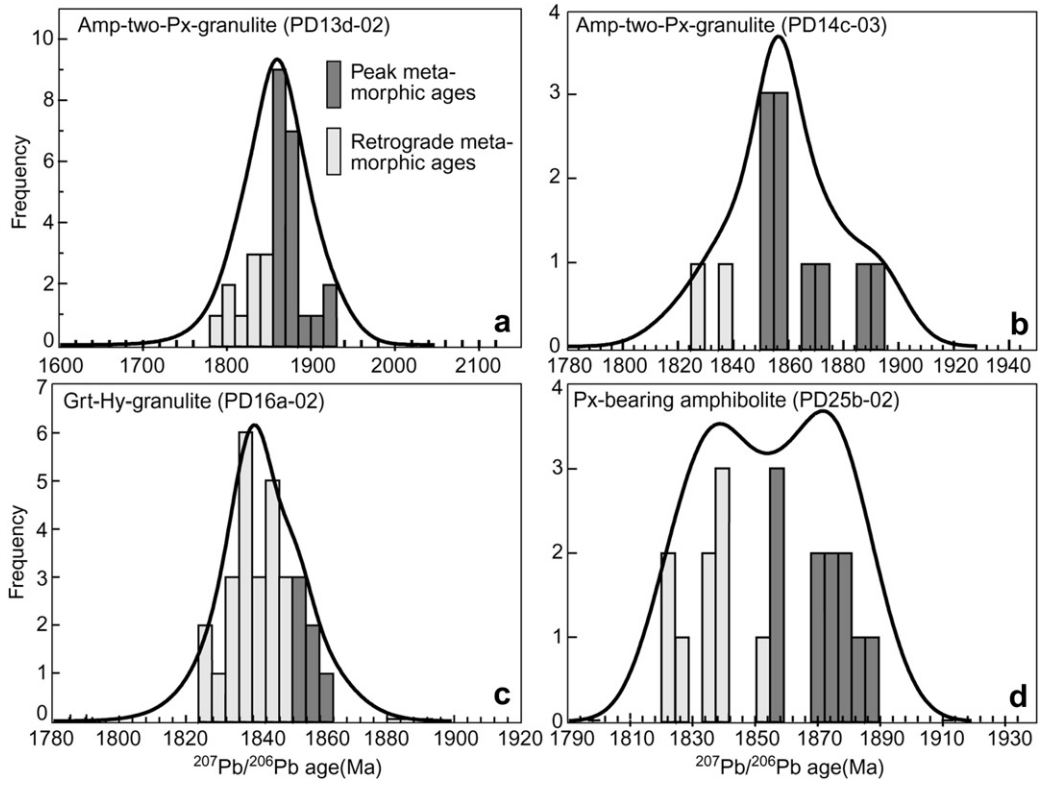

Figure 16 Histograms of $^{207}Pb/^{206}Pb$ ages of metamorphic zircons from HP granulites, Shandong Peninsula.

distinctly different from other mineral inclusions in the HP granulites mentioned above. It is possible that these zircons have been affected by later geological events. Our results emphasize the importance of laser Raman spectroscopy and electron-microprobe techniques in identifying mineral inclusions in zircons that are used for U-Pb age determination.

7.3. HP granulite facies metamorphic ages

Several investigations have been carried out on zircon U-Pb dating of the HP granulites and related rocks in the Shandong Peninsula (Table 7), but the ages of the peak HP granulite facies and the retrograde metamorphism remain controversial. Some researchers consider that the metamorphic age of the basement rocks in Shandong Peninsula is between 1950 and 1850 Ma (Wan et al., 2006; Zhou J.B. et al., 2008; Zhou X.W. et al., 2008; Tam et al., 2011), whereas others suggest that regional metamorphism in the peninsula took place between 1850 and 1800 Ma (Tang et al., 2007). In this study, HP granulite facies mineral inclusions of Grt + Cpx + Pl + Rt + Qtz have been identified in some metamorphic zircon domains. The $^{207}Pb/^{206}Pb$ ages recorded by the zircon domains with HP granulite facies inclusions in PD-13d-02; (Amp-two-Px-granulite) range from 1925 ± 27 to 1853 ± 21 Ma with a weighted mean age of 1872 ± 12 Ma; $^{207}Pb/^{206}Pb$ ages of inclusion-bearing zircons in PD-16a-02 (Grt-Hy-granulite) range from 1861 ± 9 to 1852 ± 6 Ma with a weighted mean age of 1854 ± 11 Ma; ages of zircons in PD-22a-28 (Grt-amphibolite) range from 1920 ± 92 to 1853 ± 45 Ma; ages recorded from PD-25b-02 (Amp-two-Px-granulite) range from 1928 ± 57 to 1852 ± 18 Ma with a weighted mean age of 1871 ± 8 Ma; ages from PD-14c-03 (Py-bearing amphibolite) range from 1894 ± 10 to 1853 ± 10 Ma with a weighted mean age of 1866 ± 11 Ma. Combined with the previous geochronological data, our results confirm that the HP granulite facies metamorphism in Shandong Peninsula took place between 1900 and 1850 Ma (Fig. 16).

7.4. Retrograde metamorphic ages

Grt-Hy-granulite (PD-16a-02) and Grt-amphibolite (PD-22a-28) contain retrograde metamorphic zircon domains with mineral inclusions such as orthopyroxene and amphibole. $^{207}Pb/^{206}Pb$ ages of the metamorphic zircons in PD-16a-02 range from 1849 ± 11 to 1825 ± 10 Ma with a weighted mean age of 1839 ± 3 Ma. The $^{207}Pb/^{206}Pb$ metamorphic zircon ages in PD-22a-28 range from 1849 ± 6 to 1817 ± 13 Ma with a weighted mean age of 1838 ± 5 Ma. In the three other HP granulite samples dated, zircons lack retrograde mineral inclusions, but, zircon domain ages of 1840–1820 Ma also imply a retrograde metamorphic event.

Previous investigations indicate that there are mafic and pelitic HP granulites in the Early Precambrian metamorphic basement of Shandong Peninsula. Metamorphic zircons in (Amp)-two-Px-granulite and Grt-amphibolite contain HP granulite facies mineral inclusions of Grt + Cpx + Pl + Rt + Qtz that record HP granulite facies metamorphism of the Early Precambrian metamorphic basement of the Shandong Peninsula in the Late Palaeoproterozoic.

Our integrated study involving laser Raman analysis of mineral inclusions, CL imaging and in-situ U-Pb dating of zircons, shows that HP granulite facies metamorphism in Shandong Peninsula occurred between 1900 and 1850 Ma, when protolith rocks of these rocks were subducted to ~55 km (Liu et al., 2010). Metamorphic zircons from their host TTG gneisses record not only the metamorphic event (Jahn et al., 2008; Zhou J.B. et al., 2008; Liu et al., 2011) of the Late Neoarchean (~2500 Ma) but also a HP granulite facies metamorphic event of 1900–1850 Ma. On the other hand, the retrograde metamorphic ages of the HP granulites range from 1840 to 1820 Ma, indicating the time that these rocks were exhumed to depths of ~25 km (Liu et al., 2010) where they were overprinted by medium to low-pressure granulite facies recrystallization. The youngest age recorded by the metamorphic zircons is ~1810 Ma, possibly indicating the time that the retrogressive HP granulites were uplifted to depths of 15–20 km (Liu et al., 2010) where they further recrystallized under amphibolite facies conditions.

Acknowledgements

We thank Ling Yan, Xianhua Li, Qiuli Li, Chunyan Dong, Lilin Du, Biao Song, Ziran Zhao, Huaimin Xue and Jinguang Wang for help and discussion. This study was financially supported by National Program on Key Basic Research Project (973 Program) (Grant No. 2012CB416603), the National Natural Science Foundation of China (Grant Nos. 40725007 and 40921001) and the China Geological Survey Program (Grant Nos. 1212011120150 and 1212010811065). We also thank Prof. M. Santosh and Dr. Guochun Zhao for their constructive comments and editorial corrections.

References

Ashwal, L.D., Tucker, R.D., Zinner, E.K., 1999. Slow cooling of deep crustal granulites and Pb-loss in zircon. Geochimica et Cosmochimica Acta 63 (18), 2839–2851.

Bai, W.J., Zhou, M.F., Hu, X.F., Cai, Y.C., Zhen, X.H., 1993. Mafic/Ultramafic Magmatism and Tectonic Evolution of the Northern China Craton. Sesimological Publishing House, Beijing, pp. 71–80 (in Chinese).

Black, L.P., Kamo, S.L., Allen, C.M., Aleinikoff, J.N., Davis, D.W., Korsch, R.J., Foudoulis, C., 2003. TEMORA 1: a new zircon standard for Phanerozoic U-Pb geochronology. Chemical Geology 200 (1–2), 155–170.

Geng, Y.S., Ji, C.L., 1994. Metamorphic evolution of garnet mafic granulite in the Tongyanghe region of Huai'an County, Hebei Province. In: Geological Evolution of Granulite Facies Zone in Northern North China. Sesimological Publishing House, Beijing, pp. 88–99 (in Chinese).

Guo, J.H., Zhai, M.G., Zhang, Y.G., Li, Y.G., Yan, Y.H., Zhang, W.H., 1993. Early Precambrian Manjinggou high-pressure granulite melange belt on the south edge of the Huai'an complex, North China Craton: geological features, petrology and isotopic geochronology. Acta Petrologica Sinica 9 (4), 329–341 (in Chinese with English abstract).

Guo, J.H., Zhai, M.G., Li, Y.G., Yan, Y.H., 1998. Contrasting metamorphic *p-T* paths of Archaean high-pressure granulites from the North China Craton: metamorphism and tectonic significance. Acta Petrologica Sinica 14 (4), 430–438 (in Chinese with English abstract).

Guo, J.H., O'Brien, P.J., Zhai, M.G., 2002. High-pressure granulites in the Sanggan area, North China Craton: metamorphic evolution, *p-T* paths and geotectonic significance. Journal of Metamorphic Geology 20 (8), 741–756.

Guo, J.H., Sun, M., Chen, F.K., Zhai, M.G., 2005. Sm-Nd and SHRIMP U-Pb zircon geochronology of high-pressure granulites in the Sanggan area, North China Craton: timing of Paleoproterozoic continental collision. Journal of Asian Earth Sciences 24 (5), 629–642.

Guo, S.S., Li, S.G., 2009. SHRIMP zircon U-Pb ages for the Paleoproterozoic metamorphic-magmatic events in the southeast margin of the North China Craton. Science in China Series D: Earth Sciences 52 (8), 1039–1045.

Hu, B., Zhai, M.G., Li, T., Li, Z., Peng, P., Guo, J., Kusky, T.M., 2012. Mesoproterozoic magmatic events in the eastern North China Craton and their tectonic implications: geochronological evidence from detrital zircons in the Shandong Peninsula and North Korea. Gondwana Research. http://dx.doi.org/10.1016/j.gr.2012.03.005.

Jahn, B.M., Liu, D.Y., Wan, Y.S., Song, B., Wu, J.S., 2008. Archean crustal evolution of the Jiaodong Peninsula, China, as revealed by zircon SHRIMP geochronology, elemental and Nd-isotope geochemistry. American Journal of Science 308 (3), 232–269.

Kröner, A., Wilde, S.A., Li, J.H., Wang, K.Y., 2005. Age and evolution of a late Archean to Paleoproterozoic upper to lower crustal section in the Wutaishan/Hengshan/Fuping terrain of northern China. Journal of Asian Earth Sciences 24 (5), 577–595.

Kröner, A., Wilde, S.A., Zhao, G.C., O'Brien, P.J., Sun, M., Liu, D.Y., Wan, Y.S., Liu, S.W., Guo, J.H., 2006. Zircon geochronology and metamorphic evolution of mafic dykes in the Hengshan Complex of northern China: evidence for late Palaeoproterozoic extension and subsequent high-pressure metamorphism in the North China Craton. Precambrian Research 146, 45–67.

Li, S.Z., Zhao, G.C., 2007. SHRIMP U-Pb zircon geochronology of the Liaoji granitoids: constraints on the evolution of the Paleoproterozoic Jiao-Liao-Ji belt in the Eastern Block of the North China Craton. Precambrian Research 158 (1–2), 1–16.

Li, S.Z., Zhao, G.C., Zhang, J., Sun, M., Zhang, G.W., Luo, D., 2010. Deformational history of the Hengshan-Wutai-Fuping belt: implications for the evolution of the Trans-North China Orogen. Gondwana Research 18, 611–631.

Li, X.H., Liu, Y., Li, Q.L., Guo, C.H., Chamberlain, K.R., 2009. Precise determination of Phanerozoic zircon Pb/Pb age by multi-collector SIMS without external standardization. Geochemistry Geophysics Geosystems 10 (4), 1–21.

Li, X.P., Guo, J.H., Zhao, G.C., Li, H.K., Song, Z.H., 2011. Formation of the Paleoproterozoic calc-silicate and high-pressure mafic granulite in the Jiaobei terrane, eastern Shandong, China. Acta Petrologica Sinica 27, 961–968 (in Chinese with English abstract).

Li, Y.G., Zhai, M.G., Liu, W.J., 1997. Sm-Nd geochronology of the high-pressure basic granulite, in Laixi, eastern Shandong. Scientia Geologica Sinica 32 (3), 283–290 (in Chinese with English abstract).

Liu, F.L., Shen, Q.H., Zhao, Z.R., Katayama, I., 2002. Identification of high-pressure mineral assemblages in garnet mafic granulites, northwestern Hebei Province: evidence from mineral inclusions in zircons. Acta Geologica Sinica 27 (4), 209–216 (in Chinese with English abstract).

Liu, J.H., Liu, F.L., Liu, P.H., Wang, F., Ding, Z.J., 2011. Polyphase magmatic events from Early Precambrian metamorphic basement in Jiaobei area: evidences from the zircon U-Pb dating of TTG and granitic gneisses. Acta Petrologica Sinica 26 (7), 943–960 (in Chinese with English abstract).

Liu, P.H., Liu, F.L., Wang, F., Liu, J.H., 2010. Genetic mineralogy and metamorphic evolution of mafic high-pressure (HP) granulites from the Shandong Peninsula, China. Acta Petrologica Sinica 26 (7), 2039–2056 (in Chinese with English abstract).

Liu, W.J., Zhai, M.G., Li, Y.G., 1998. Metamorphism of the high-pressure basic granulite in Laixi, Eastern Shandong, China. Acta Petrologica Sinica 14 (4), 449–459 (in Chinese with English abstract).

Luo, Y., Sun, M., Zhao, G.C., Li, S.Z., Ayers, J.C., Xia, X.P., Zhang, J.H., 2008. A comparison of U-Pb and Hf isotopic compositions of detrital zircons from the North and South Liaohe groups: constraints on the evolution of the Jiao-Liao-Ji Belt, North China Craton. Precambrian Research 163 (3–4), 279–306.

Lu, L.Z., Xu, X.C., Liu, F.L., 1996. Early Precambrian Khondalite Series in North China. Changchun Publishing House, Changchun (in Chinese).

Ma, J., Wang, R.M., 1995. The discovery of coexisting kyanite + perthite assemblage in Xuanhua-Chicheng high-pressure granulite belt and its geological significance. Acta Petrologica Sinica 11 (3), 273–278 (in Chinese with English abstract).

Miao, L.C., Luo, Z.K., Guan, K., Huang, J.Z., 1998. The implications of the SHRIMP U-Pb age in zircon to the petrogenesis of the Linglong granite, East Shandong Province. Acta Petrologica Sinica 14 (2), 198–206 (in Chinese with English abstract).

O'Brien, P.J., Walte, N., Li, J.H., 2005. The petrology of two distinct granulite types in the Hengshan Mts, China, and tectonic implications. Journal of Asian Earth Sciences 24 (5), 615–627.

Roberts, M.P., Finger, F., 1997. Do U-Pb zircon ages from granulites reflect peak metamorphic conditions? Geology 25 (4), 319–322.

Song, B.K., Zhang, H.Y., Wan, Y.S., Jian, P., 2002. Mount making and procedure of the SHRIMP dating. Geological Review 48 (Supp.), 26–30 (in Chinese with English abstract).

Tam, P.Y., Zhao, G.C., Liu, F.L., Zhou, X.W., Sun, M., Li, S.Z., 2011. Timing of metamorphism in the Paleoproterozoic Jiao-Liao-Ji Belt: new SHRIMP U-Pb zircon dating of granulites, gneisses and marbles of the Jiaobei massif in the North China Craton. Gondwana Research 19 (1), 150–162.

Tam, P.Y., Zhao, G.C., Zhou, X.W., Guo, J.H., Sun, M., Li, S.Z., Yin, C.Q., Wu, M.L., 2012. Metamorphic P-T path and implications of high-pressure pelitic granulites from the Jiaobei massif in the Jiao-Liao-Ji Belt, North China Craton. Gondwana Research. doi: 10.1016/j.gr.2011.09.006.

Tang, J., Zheng, Y.F., Wu, Y.B., Gong, B., Liu, X.M., 2007. Geochronology and geochemistry of metamorphic rocks in the Jiaobei terrane: constraints on its tectonic affinity in the Sulu orogen. Precambrian Research 152 (1–2), 48–82.

Timmermann, H., Štědrá, V., Gerdes, A., Noble, S.R., Parrish, R.R., Dorr, W., 2004. The problem of dating high-pressure metamorphism: a U-Pb isotope and geochemical study on eclogites and related rocks of the Mariánské Lázně Complex, Czech Republic. Journal of Petrology 45 (7), 1311–1338.

Vavra, G., Gebauer, D., Schmid, R., Compston, W., 1996. Multiple zircon growth and recrystallization during polyphase Late Carboniferous to Triassic metamorphism in granulites of the Ivrea Zone (Southern Alps): an ion microprobe (SHRIMP) study. Contributions to Mineralogy and Petrology 122 (4), 337–358.

Wan, Y.S., Song, B., Liu, D.Y., Wilde, S.A., Wu, J.S., Shi, Y.R., Yin, X.Y., Zhou, H.Y., 2006. SHRIMP U-Pb zircon geochronology of Palaeoproterozoic metasedimentary rocks in the North China Craton: evidence for a major Late Palaeoproterozoic tectonothermal event. Precambrian Research 149 (3–4), 249–271.

Wan, Y.S., Dong, C.Y., Wang, W., Xie, H.Q., Liu, D.Y., 2010. Archean basement and a paleoproterozoic collision orogen in the Huoqiu area at the southeastern margin of North China Craton: evidence from sensitive high resolution ion micro-probe U-Pb zircon geochronology. Acta Geologica Sinica 84 (1), 91–104.

Wang, L.G., Qiu, Y.M., McNaughton, N.J., Groves, D.I., Luo, Z.K., Huang, J.Z., Miao, L.C., Liu, Y.K., 1998. Constraints on crustal evolution and gold metallogeny in the Northwestern Jiaodong Peninsula, China, from SHRIMP U-Pb zircon studies of granitoids. Ore Geology Reviews 13 (1), 275–291.

Wang, P.C., An, J.T., 1996. Main achievement and progress of the basic geological research over last ten years in eastern Shandong region. Shandong Geology 12 (1), 8–23 (in Chinese with English abstract).

Wang, R.M., Chen, Z.Z., Chen, F., 1991. Grey tonalitic gneiss and high-pressure granulite inclusions in Hengshan, Shanxi Province, and their geological significance. Acta Petrologica Sinica 4, 36–45 (in Chinese with English abstract).

Wang, S.J., Wan, Y.S., Zhang, C.J., Yang, E.X., Song, Z.Y., Wang, L.F., Wang, J.G., 2009. Forming ages of early Precambrian metamorphic strata in Shandong Province. Shandong Land and Resources 25 (10), 18–24 (in Chinese with English abstract).

Wang, F., Liu, F.L., Liu, P.H., Liu, J.H., 2010. Metamorphic evolution of early Precambrian khondalite seris in North Shandong Province. Acta Petrologica Sincia 26 (7), 2057–2072 (in Chinese with English abstract).

Wei, C.J., Zhang, C.G., Zhang, A.L., Wu, H.T., Li, J.H., 2001. Metamorphic *p-T* conditions and geological significance of high-pressure granulite from the Jianping complex, western Liaoxi province. Acta Petrologica Sinica 17 (2), 269−282 (in Chinese with English abstract).

Whitehouse, M.J., Platt, J.P., 2003. Dating high-grade metamorphism-constraints from rare-earth elements in zircon and garnet. Contributions to Mineralogy and Petrology 145 (1), 61−74.

Whitney, D.L., Evans, B.W., 2010. Abbreviations for names of rock-forming minerals. American Mineralogist 95 (1), 185−187.

Yin, C.Q., Zhao, G.C., Guo, J.H., Sun, M., Zhou, X.W., Zhang, J., Xia, X.P., Liu, C.H., 2011. U-Pb and Hf isotopic study of zircons of the Helanshan Complex: constrains on the evolution of the Khondalite Belt in the Western Block of the North China Craton. Lithos 122, 25−38.

Yin, C.Q., Zhao, G.C., Sun, M., Xia, X.P., Wei, C.J., Zhou, X.W., Leung, W.H., 2009. LA-ICP-MS U-Pb zircon ages of the Qianlishan Complex: constrains on the evolution of the Khondalite Belt in the Western Block of the North China Craton. Precambrian Research 174, 78−94.

Zhai, M.G., Guo, J.H., Yan, Y.H., Han, X.L., Li, Y.G., 1992. Discovery and preliminary study of Archaean high-pressure mafic granulites in North China. Science in China: Series B 22 (12), 1325−1330 (in Chinese with English abstract).

Zhai, M.G., Guo, J.H., Li, Y.G., 1994. High-pressure mafic granulite zone and related rock association in Jin-Ji-Inner Mongolia joint area. In: Geological Evolution of Granulite Facies Zone in Northern North China. Sesimological Publishing House, Beijing, pp. 21−31 (in Chinese).

Zhai, M.G., 2004. 2.1 ∼ 1.7 Ga geological event group and it s geotectonic significance. Acta Petrologica Sinica 20 (6), 1343−1354 (in Chinese with English abstract).

Zhai, M.G., 2009. Two kinds of granulites (HT-HP and HT-UHP) in North China Craton: their genetic relation and geotectonic implications. Acta Petrologica Sinica 25 (8), 1753−1771 (in Chinese with English abstract).

Zhai, M.G., Santosh, M., 2011. The early Precambrian odyssey of the North China Craton: a synoptic overview. Gondwana Research 20, 6−25.

Zhang, J., Zhao, G.C., Sun, M., Wilde, S.A., Li, S.Z., Liu, S.W., 2006a. High-pressure mafic granulites in the Trans-North China Orogen: tectonic significance and age. Gondwana Research 9, 349−362.

Zhang, H.F., Zhai, M.G., Peng, P., 2006b. Zircon SHRIMP U-Pb age of the Paleoproterozoic high-pressure granulites from the Sanggan area, the North China Craton and its geologic implications. Earth Science Frontiers 13 (3), 190−199 (in Chinese with English abstract).

Zhao, G.C., Cawood, P.A., Wilde, S.A., Lu, L.Z., 2001. High-pressure granulites (retrograded eclogites) from the Hengshan Complex, North China Craton: petrology and tectonic implications. Journal of Petrology 42 (6), 1141−1170.

Zhao, G.C., 2001. Paleoproterozoic assembly of the North China Craton. Geological Magazine 138, 87−91.

Zhao, G.C., Sun, M., Wilde, S.A., Li, S.Z., 2003. Assembly, accretion and breakup of the Paleo-Mesoproterozoic Columbia Supercontinent: records in the North China Craton. Gondwana Research 6 (3), 417−434.

Zhao, G.C., Sun, M., Wilde, S.A., Li, S.Z., 2005. Late Archean to Paleoproterozoic evolution of the North China Craton: key issues revisited. Precambrian Research 136 (2), 177−202.

Zhao, G.C., 2009. Metamorphic evolution of major tectonic units in the basement of the North China Craton: key issues and discussion. Acta Petrologica Sinica 25 (8), 1772−1792.

Zhao, G.C., He, Y.H., Sun, M., 2009. The Xiong'er volcanic belt at the southern margin of the North China Craton: petrographic and geochemical evidence for its outboard position in the Paleo-Mesoproterozoic Columbia Supercontinent. Gondwana Research 16 (2), 170−181.

Zhao, G.C., Wilde, S.A., Guo, J.H., Cawood, P.A., Sun, M., Li, X.P., 2010. Single zircon grains record two Paleoproterozoic collisional events in the North China Craton. Precambrian Research 177 (3−4), 266−276.

Zhao, G.C., Li, S.Z., Sun, M., Wilde, S.A., 2011. Assembly, accretion, and break-up of the Palaeo-Mesoproterozoic Columbia supercontinent: rock record in the North China Craton revisited. International Geology Review 9 (1), 1−18.

Zhou, J.B., Wilde, S.A., Zhao, G.C., Zheng, C.Q., Jin, W., Zhang, X.Z., Cheng, H., 2008a. SHRIMP U-Pb zircon dating of the Neoproterozoic Penglai Group and Archean gneisses from the Jiaobei Terrane, North China, and their tectonic implications. Precambrian Research 160 (3−4), 323−340.

Zhou, X.W., Wei, C.J., Dong, Y.S., Lu, L.Z., 2003. Characteristics and genetic implications of diffusion zoning in garnet from Al-rich series of the Jingshan group in north Jiaodong. Acta Petrologica Sinica 19 (4), 752−760 (in Chinese with English abstract).

Zhou, X.W., Wei, C.J., Geng, Y.S., Zhang, L.F., 2004. Discovery and implications of the high-pressure pelitic granulites from the Jiaobei massif. Chinese Science Bulletin 49 (14), 1942−1948 (in Chinese with English abstract).

Zhou, X.W., Wei, C.J., Geng, Y.S., 2007. Phase equilibria *p-T* path of the high- and low-pressure pelitic granulites from the Jiaobei massif. Earth Science Frontiers 14 (1), 135−143 (in Chinese with English abstract).

Zhou, X.W., Zhao, G.C., Wei, C.J., Geng, Y.S., Sun, M., 2008b. EPMA U-Th-Pb monazite and SHRIMP U-Pb zircon geochronology of high-pressure pelitic granulites in the Jiaobei massif of the North China Craton. American Journal of Science 308 (3), 328−350.

Zhou, X.W., Zhao, G.C., Geng, Y.S., 2010. Helanshan high-pressure pelitic granulites: petrological evidence for collision event in the Western Block of the North China Craton. Acta Petrological Sinica 26, 2113−2121.